Invasion and maintenance of spore killers in populations of ascomycete fungi

Ivain Martinossi-Allibert[1], Carl Veller[2], S. Lorena Ament-Velásquez[1], Aaron A. Vogan[1], Claus Rueffler*[3], Hanna Johannesson*[1], and [2]

[1]Department of Organismal Biology, Uppsala University, Sweden

[2]Department of Organismic and Evolutionary Biology, Harvard University, USA

[3]Department of Ecology and Genetics, Animal Ecology, Uppsala University, Sweden

*Both authors contributed equally

June 30, 2020

keywords: spore killer, meiotic drive, ascomycete fungi, meiosis, population genetics.

Abstract

Meiotic drivers are selfish genetic elements that have the ability to become over-represented among the products of meiosis. This transmission advantage makes it possible for them to spread in a population even when they impose fitness costs on their host organisms. Whether a meiotic driver can invade a population, and subsequently reach fixation or coexist in a stable polymorphism, depends on the one hand on the biology of the host organism, including its life-cycle, mating system, and population structure, and on the other hand on the specific fitness effects of the driving allele on the host. Here, we present a population genetics model for spore killing, a type of drive specific to fungi. We show how ploidy level, rate of selfing, and efficiency of spore killing affect the invasion probability of a driving allele and the conditions for its stable coexistence with the non-driving allele. Our model can be adapted to different fungal life-cycles, and is applied here to two well-studied genera of filamentous ascomycetes known to harbor spore killing elements, *Podospora* and *Neurospora*. We discuss our results in the light of recent empirical findings for these two systems.

1 Introduction

Our understanding of population genetics relies on the expectation that the two copies of a gene in a diploid genome are represented equally among the products of meiosis — this is Mendel's first law (Lyttle, 1993). However, some genetic elements are able to distort the meiotic process and become over-represented among the meiotic products, a phenomenon called 'meiotic drive' (Sandler and Novitski, 1957; Burt and Trivers, 2009). Due to their ability to distort meiosis, meiotic drivers (MDs) gain a selective advantage at the gene level that allows them to increase in frequency in a population even when they impose fitness costs on their host organism (Hamilton, 1967; Akbari et al., 2013; Pinzone and Dyer, 2013; Kyrou et al., 2018). The ensuing genetic conflict between a MD and its host can affect many evolutionary processes (Rice, 2013). For example, rapid co-evolution between MDs and counteracting genes, called suppressors, can accelerate speciation by creating genetic incompatibilities between recently separated populations (Frank, 1991), as well as shape genetic architecture in other important ways (Henikoff et al., 2001; Hurst and Werren, 2001; Werren, 2011). MDs can also affect mating behavior, since their spread can be impeded by, for example, inbreeding (Hurst and Werren, 2001; Bull et al., 2019) and multiple mating (Haig and Bergstrom, 1995).

MDs were discovered as early as 1928 (Sandler and Novitski, 1957) and have been studied extensively since then. Early empirical observations were closely followed by theoretical work aimed at understanding the unique behavior of these selfish genetic elements (see for example Hiraizumi, 1962; Lewontin and Dunn, 1960; Lewontin, 1968, on the *t-haplotype* in mice). Theoretical work has focused on two key aspects of meiotic drive dynamics: under what conditions can a MD (i) invade a population and (ii) coexist at a stable equilibrium with a non-driving allele? These questions have been investigated with reference to a wide variety of species harboring MDs (e.g. Lewontin and Dunn, 1960; Fishman and Kelly, 2015; Brand et al., 2015; Hall and Dawe, 2018), which has revealed some general patterns of MD dynamics. First, since MDs are over-represented among successful meiotic products, theory predicts that, in the absence of counteracting forces, they should increase in frequency and reach fixation. However, the presence of suppressor alleles or fitness costs associated with the MD can bring the invasion process to a halt, leading ultimately to either the loss of the MD or prolonged coexistence with a non-driving allele. The presence of strong recessive fitness costs to the MD appears as a typical condition for coexistence, allowing invasion of the MD but not fixation (e.g. Fishman and Kelly, 2015; Lewontin and Dunn, 1960; Holman et al., 2015). These general principles, however, are far from encompassing the complexity and diversity of MD dynamics. Indeed, although all MDs distort Mendelian proportions, the

diversity of their modes of action as well as the details of the life cycle of each host make insights from one species often not applicable to others. In order to position our work in the context of the meiotic drive literature, we give a brief overview of drive mechanisms in the following paragraphs.

Mechanisms of drive can be classified into three types: female drive, male drive, and spore killing (reviewed in Burt and Trivers, 2009; Lindholm et al., 2016). Female drive, as observed in maize *Zea mays* (Buckler et al., 1999), the monkeyflower *Mimulus guttatus* (Fishman and Saunders, 2008), and the house mouse *Mus musculus* (Didion et al., 2015), takes advantage of the asymmetry of female meiosis by preferentially segregating the driving element to the functional egg cell (or macrospore). In contrast, in male drive the MD acts by killing the meiotic products (male gametes) that carry a different allele. Examples are the *t-haplotype* in *Mus musculus* (Silver, 1985) and *SD* in *Drosophila melanogaster* (Larracuente and Presgraves, 2012). The mechanism of spore killing in fungi is similar to male drive in that meiotic products that do not carry the MD are killed, thus reducing the number of meiotic products in heterozygotes (Raju, 1994). Spore killing differs from male drive in that it affects all individuals in the population (instead of being restricted to gametogenesis in one sex). Spore killing MDs were first described in *Podospora anserina* (Padieu and Bernet, 1967), and later in other species, including the genus *Neurospora* (Turner and Perkins, 1979), as well as the fission yeast *Schizosaccharomyces pombe* (Zanders et al., 2014). The three drive mechanisms described above differ in the type of selective advantage and in the nature of the costs they impose on their hosts. In female drive, the MD preferentially takes the place of the alternative allele in the egg, without (necessarily) reducing the number of eggs produced. As a consequence, female drive can impose little or no costs to its host, while the MD increases in absolute number of copies (i.e., it *replaces* the alternative allele). Such MDs have therefore been termed *absolute* drivers (Lyttle, 1991). In contrast, male drive and spore killing can result in only a relative increase of the MD, because meiotic products carrying the alternative allele are killed and not necessarily replaced. Male drive and spore killing can therefore be referred to as *relative* drive (Lyttle, 1991). They impose fitness costs to their host in part because the total number of meiotic products is reduced. These costs are expected to be more important in spore killing because meiotic products of fungi are offspring (spores) and not gametes. It is important to note that the elimination of meiotic products in male drive may not always result in a purely relative type of drive. Indeed, because a large number of gametes (sperm or pollen) have to compete to fertilize a small number of eggs, a reduction in gamete count does not immediately imply a reduction in male fertility (Hartl, 1972). Depending on the mating system, male drive can be purely absolute if each female mates exclusively with a single male and the reduction in sperm count does not affect male fertility, or purely relative if post-copulatory competition is so

intense that male reproductive success is reduced proportionally to the rate of sperm killing.

An important factor in male drive and spore killing is the possibility that the killing of some proportion of the meiotic products (gametes or spores) that do not carry the MD can provide an absolute fitness benefit to the surviving ones. In the remainder of this study, we refer to such a potential fitness benefit as *killing advantage*. In male drive, killing advantage can result from compensatory mechanisms in the host that reduce the loss in reproductive success resulting from the action of the MD. Such a killing advantage can occur through the production of additional gametes, which partially compensates for the loss caused by the gamete killing MD. Compensation of this kind has been observed, for example, in the stalk-eyed fly *Teleopsis dalamanni* (Meade et al., 2019), and can be viewed as an adaptive response of the host. Importantly, the gamete killer itself can benefit from this killing advantage due to an increase in the absolute number of gametes, including those carrying the MD. Thus, a killing advantage causes a male driver to be more of an absolute driver. In Box 1 we compare how purely relative male drive, male drive with killing advantage and female drive differ in terms of their selective advantage and invasion dynamics. The selective advantage of purely relative male drive is positively frequency-dependent, and this advantage is therefore minimal at low frequency during the early stage of invasion (as pointed out by Nauta and Hoekstra, 1993). Absolute drivers and female or male drivers with killing advantage, on the other hand, have a higher initial selective advantage because they increases in absolute copy number when driving. This distinction suggests that it is important to identify to which degree a spore killer acts as a relative or absolute drive in order to predict the population dynamics of the driver.

At first glance, spore killing appears to be a purely relative drive. Contrary to male drive, where the MD is eliminating gametes with an unclear effect on the fitness of the host, spore killers in fungi are directly eliminating some proportion of their host's offspring. However, several mechanisms may exist that could allow a spore killer to derive an absolute fitness advantage from killing, and in what follows we propose two possible scenarios. First, a killing advantage could arise if the host can reallocate energy made available from the aborted development of 'killed' spores to the production of additional spores or to providing surviving spores with additional resources. Second, a killing advantage could also arise under local resource competition among sibling spores. In this case, killing would provide surviving spores with a fitness advantage in the form of additional resources available for growth (Nauta and Hoekstra, 1993; Lindholm et al., 2016). In both scenarios, the killing advantage provides the spore killer with a fitness benefit that makes it more akin to an absolute drive mechanism.

In the present study, we develop a single-locus population genetics model of a spore killing

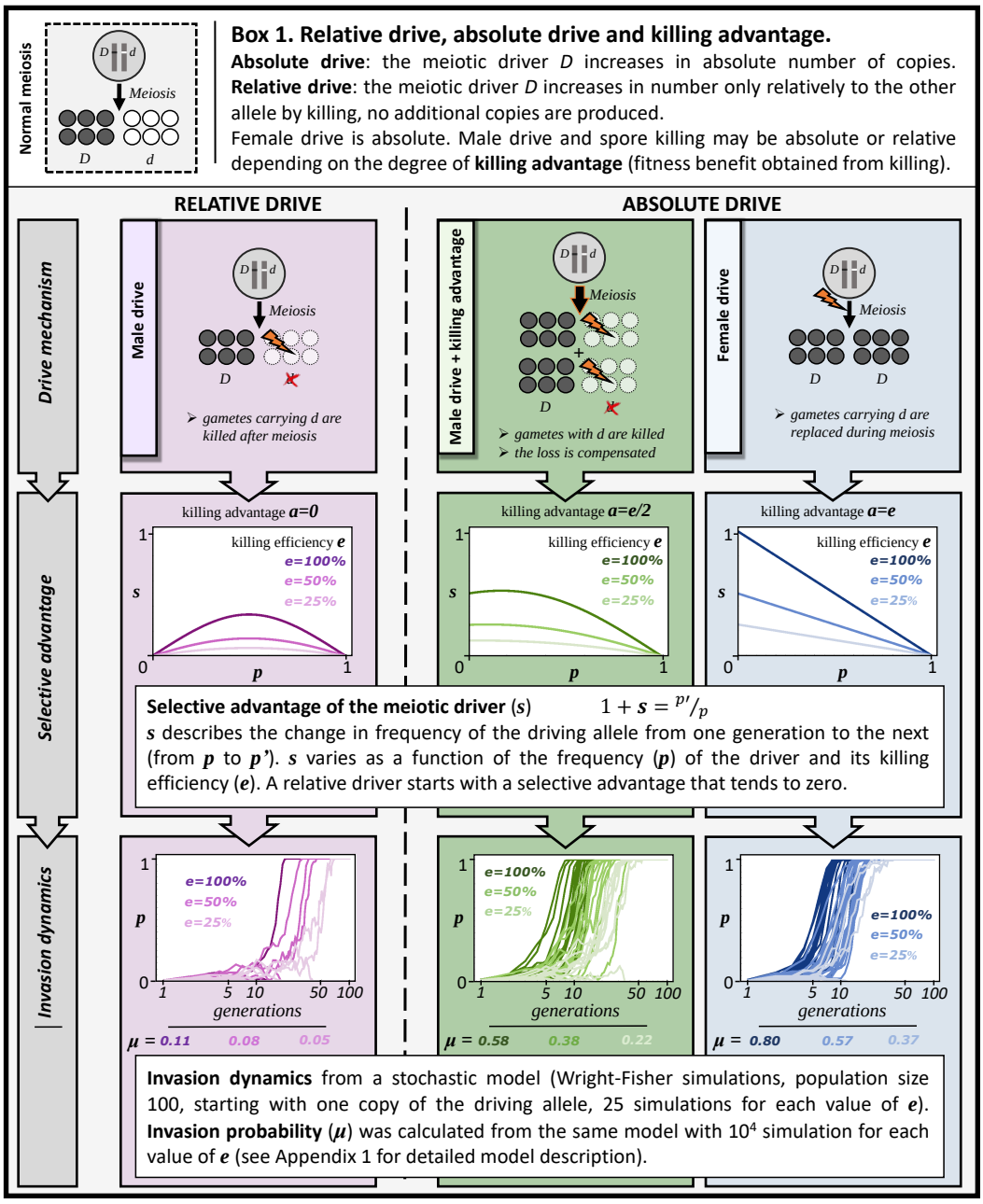

MD in an ascomycete fungi host based on the life cycles of *Podospora anserina* and heterothallic *Neurospora* species. We find that killing advantage is a crucial parameter determining the invasion success of a spore killer MD, especially in small populations where drift is important. Nevertheless, a spore killer without killing advantage can invade more frequently than a neutral allele, and this invasion probability should also be highly dependent on mutational input and the likelihood of suppression. In the absence of selfing, incomplete killing efficiency of the spore killer and some fitness costs are necessary for stable coexistence with a non-killer allele to be possible. When the selfing rate is higher, however, coexistence is possible even with fully efficient killing. As in other

drive systems, recessive fitness costs facilitate coexistence, but we also find that killing advantage allows for coexistence in the case of additive fitness costs. The range of parameters allowing for coexistence also depends on the stage of the life cycle at which the MD's fitness costs are expressed. In light of empirical data, our model suggests that the observed spore killer frequencies in natural populations of *Podospora* and *Neurospora* could be explained by recessive costs of the spore killer combined with high selfing rates in *Podospora*.

2 The model

We study a diploid, single-locus, two-allele population genetics model in discrete time with non-overlapping generations. The two alleles are the spore killer allele D and the sensitive non-killing allele d. The modelled life cycles correspond to those of filamentous ascomycetes of the genera *Podospora* and *Neurospora*. Both taxa are model systems in fungal genetics and harbor spore killing elements (e.g. Silar, 2013; Vogan et al., 2019; Svedberg et al., 2020). Moreover, the life cycle of *Neurospora* is representative for many other filamentous ascomycetes. We first assume that the population is sufficiently large that drift can be ignored. Under this assumption, we determine the parameter combinations that permit invasion of the spore killer allele D, and then ask under what further conditions invasion results in fixation of D or stable coexistence of D and d. We then relax the assumption of infinitely large population size and explore the role of drift in the early phase of invasion of D by means of a Wright-Fisher model.

2.1 Life cycle and recursion equations

Figure 1 shows a schematic view of the life cycle of *P. anserina* from which we derive a set of recursion equations describing the change in frequency of the spore killer allele D across one generation. The life cycle starts at meiosis (left panel of Figure 1), which occurs in ascomycete fungi shortly after formation of the diploid zygote. Each diploid cell undergoes meiosis followed by one mitosis, resulting in the formation of a single sac, or ascus, containing eight haploid nuclei. These nuclei can be packaged into pairs, forming a dikaryotic spore (two haploid nuclei in the same cytoplasm), or stay isolated, resulting in the formation of a monokaryotic spore (haploid). In *P. anserina*, the frequency of monokaryotic spores is low (van der Gaag, 2005) and we assume that an ascus either contains one pair of monokaryotic spores (with probability m) or none (probability $1-m$). Heterozygote diploid cells Dd can result in the formation of either heteroallelic Dd or homoallelic DD and dd dikaryotic spores due to allelic segregation at meiosis. In the case of first-division segregation (see Figure 1) at the spore killer locus, which occurs with probability f, two

homoallelic spores of each genotype are formed, while in the case of second-division segregation (probability $1-f$), four heteroallelic spores are formed. When monokaryotic spores of genotype d or dikaryotic spores of genotype dd share an ascus with spores of genotype D, DD or Dd, they are killed with probability e, which is the 'killing efficiency' of D. Dikaryotic spores of the Dd genotype are not affected by spore killing, because the D nucleus offers protection against killing to the entire spore. The frequencies of the different types of spores after meiosis are denoted by M_{DD}, M_{Dd}, M_{dd}, M_D and M_d, respectively.

After meiosis, spores germinate and form a mycelium, which is the vegetative growth stage of the life cycle. We assume that monokaryons and dikaryons do not experience different growth rates during that vegetative stage. The vegetative stage is followed by the reproductive stage, which is represented in the right panel of Figure 1. Dikaryons and monokaryons contribute to a common pool of randomly mating gametes, and dikaryons have the additional possibility to self with probability s. Selfing in *P. anserina* can only occur when a dikaryon carries nuclei of the two different mating types. We assume here that the mating-type locus always undergoes second-division segregation during meiosis, making dikaryons automatically heteroallelic for the mating-type locus so that selfing is always possible (in nature, the probability of second-division segregation of the mating-type locus is not 100% in *P. anserina* but very close, van der Gaag (2005)). As a consequence of this mating type constraint, heteroallelic dikaryons of genotype Dd can only produce heterozygote diploid zygotes Dd through selfing. At each stage of the life cycle, our model includes the possibility for fitness costs resulting in reduced viability associated with the spore killing allele D.

2.1.1 Structure of the recursions

Because of the occurrence of selfing, mating is not random in the population, and so we need to track the frequencies of the diploid genotypes DD, Dd and dd. The system can be completely described by the frequency of two genotypes, as the frequencies of the three genotypes add up to 1; however, for completeness we derive the recursions for all three genotypes. Each generation, some individuals from each genotype are produced through selfing and some through outcrossing. Thus, the change in frequency for the three genotypes DD, Dd and dd is given by

$$p'_{DD} = \Big[selfing_{DD}(p_{DD}, p_{Dd}, p_{dd}) + outcrossing_{DD}(p_{DD}, p_{Dd}, p_{dd})\Big]\frac{1}{\overline{W}} \tag{1a}$$

$$p'_{Dd} = \Big[selfing_{Dd}(p_{DD}, p_{Dd}, p_{dd}) + outcrossing_{Dd}(p_{DD}, p_{Dd}, p_{dd})\Big]\frac{1}{\overline{W}} \tag{1b}$$

$$p'_{dd} = \Big[selfing_{dd}(p_{DD}, p_{Dd}, p_{dd}) + outcrossing_{dd}(p_{DD}, p_{Dd}, p_{dd})\Big]\frac{1}{\overline{W}}, \tag{1c}$$

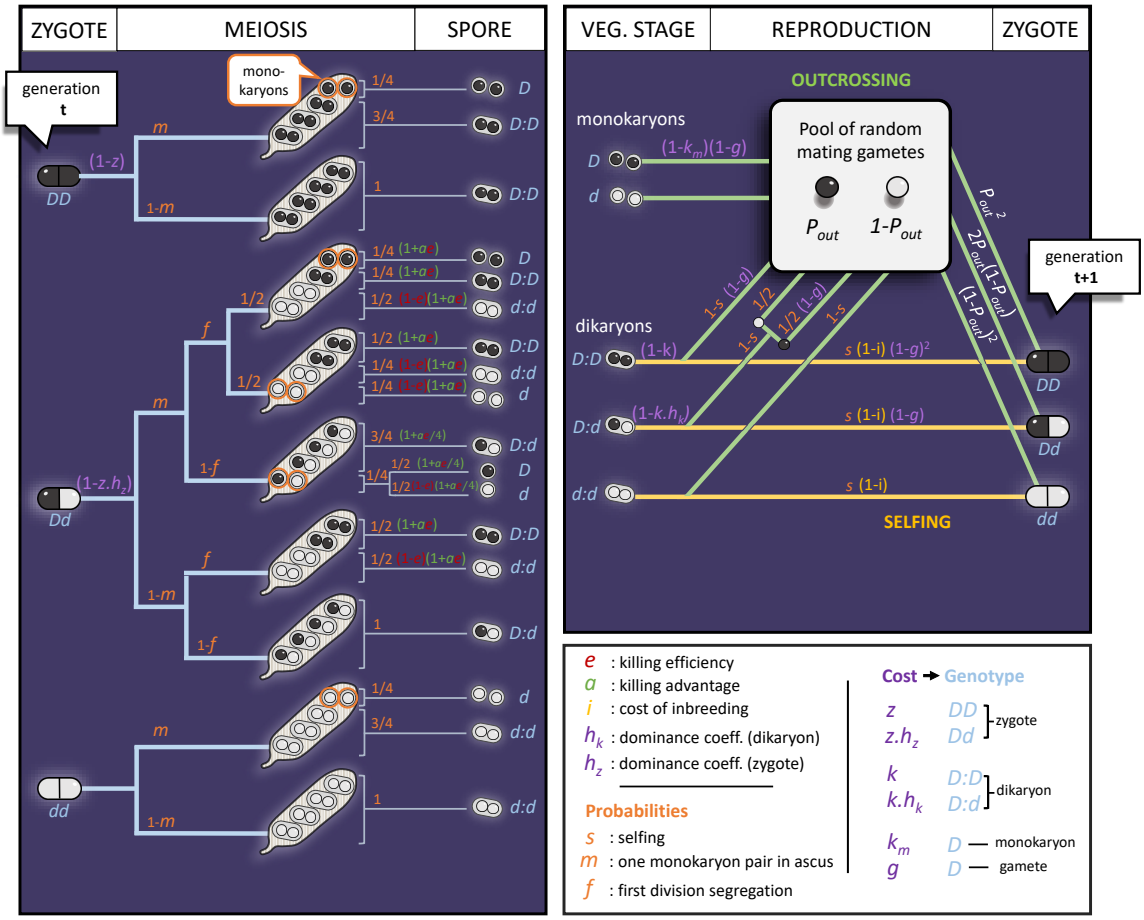

Figure 1: **Life cycle diagram of *P. anserina*.** The life cycle is presented from zygote to zygote. The left panel shows the meiosis stage occurring shortly after zygote formation and asci representing all possible segregation patterns of D and d from the three possible diploid genotypes. The right panel shows the reproductive stage with the outcrossing and selfing modes of reproduction, leading to fertilization and the formation of the diploid zygotes of the next generation. The recursion equations can be constructed by following the lines of the life cycle diagram and multiplying each genotype frequency with the costs and probabilities that apply to it. Specifically, purple symbols represent potential fitness costs associated with carrying the spore killer allele D, while orange symbols represent probabilities of alternative events (for example, selfing occurring with probability s versus outcrossing occurring with probability $1 - s$). Green symbols represent a killing advantage (a) associated with spore killing, while killing efficiency (e) is colored in red. Finally, the costs of inbreeding (i) at all loci associated with selfing is represented in yellow.

where the frequencies of a given genotype in the current and next generation are indicated by p and p' respectively, with the genotype as a subscript. We introduce the full expressions for how selfing and outcrossing contribute to the different genotype frequencies in the next section.

2.1.2 Detailed recursions

The treatment of selfing and outcrossing is inspired by a plant population genetics model with self fertilization (Holsinger et al., 1984). Beginning with the selfing part of the life cycle (right-hand panel of Figure 1), we start from the three possible dikaryotic genotypes after meiosis, M_{DD}, M_{Dd} and M_{dd}. Dikaryons may pay fitness costs if carrying one or two copies of the spore killer. If the dikaryon carries two copies, the costs are k, resulting in survival probability $1-k$. If the dikaryon carries one copy, the costs are kh_k with h_k the dominance parameter of the fitness costs, and the survival probability is $1-kh_k$. Genotype frequencies are then adjusted by the selfing probability s, and all genotypes are exposed to a selfing costs i due to inbreeding, resulting in a survival probability $1-i$. Finally, because gametes are also produced during the selfing process, individuals carrying the spore killer genotype are exposed to paying gametic costs g during selfing, resulting in the survival probabilities $(1-g)^2$ and $1-g$ for dikaryons of the DD and Dd genotypes, respectively. We can now write the selfing contribution to next generation's diploid genotype as

$$selfing_{DD} = M_{DD}(1-k)s(1-i)(1-g)^2 \tag{2a}$$

$$selfing_{Dd} = M_{Dd}(1-kh_k)s(1-i)(1-g) \tag{2b}$$

$$selfing_{dd} = M_{dd}s(1-i) \tag{2c}$$

For the outcrossing part of the life cycle, random mating is assumed. We denote by p_{out} the frequency of the spore killing allele D in the pool of randomly mating gametes. It is important to note that p_{out} only represents a frequency within the outcrossing fraction of the total population, denoted by T_{out}. More precisely, T_{out} consists of of all gametes from monokaryotic individuals (potentially reduced due to fitness costs k_m for monokaryons carrying the D allele) together with the fraction $1-s$ of outcrossing gametes from dikaryons, all discounted by the appropriate reduction in viability due to costs. The contributions from outcrossing to the genotype frequencies at the next generation follow Hardy-Weinberg proportions and are weighted by T_{out} to represent valid frequencies in the total population,

$$outcrossing_{DD} = T_{\text{out}} \times p_{\text{out}}^2 \tag{3a}$$

$$outcrossing_{Dd} = T_{\text{out}} \times 2p_{\text{out}}(1-p_{\text{out}}) \tag{3b}$$

$$outcrossing_{dd} = T_{\text{out}} \times (1-p_{\text{out}})^2 \tag{3c}$$

where

$$\begin{aligned} T_{\text{out}} &= M_D(1-k_m)(1-g) + M_d \\ &\quad + (1-s)\left(M_{DD}(1-k)(1-g) + M_{Dd}(1-kh_k)\frac{(1-g)}{2} + M_{dd}\right) \end{aligned} \tag{4a}$$

$$\begin{aligned} p_{\text{out}} &= \Big(M_D(1-k_m)(1-g) \\ &\quad + (1-s)\left(M_{DD}(1-k)(1-g) + M_{Dd}(1-kh_k)\frac{(1-g)}{2}\right)\Big)\frac{1}{T_{\text{out}}}. \end{aligned} \tag{4b}$$

The expressions for the genotype frequencies after meiosis are given by

$$M_D = \frac{m}{4}\left(p_{DD}(1-z) + p_{Dd}(1-zh_z)\left(\frac{f}{2}(1+ae) + (1-f)\frac{(1+\frac{ae}{4})}{2}\right)\right) \tag{5a}$$

$$M_d = \frac{m}{4}\left(p_{dd} + (1-e)p_{Dd}(1-zh_z)\left(\frac{f}{2}(1+ae) + (1-f)\frac{(1+\frac{ae}{4})}{2}\right)\right) \tag{5b}$$

$$M_{DD} = \left(\frac{3}{4}m + (1-m)\right)\left(p_{DD}(1-z) + p_{Dd}(1-zh_z)\frac{f}{2}(1+ae)\right) \tag{5c}$$

$$M_{Dd} = \left(\frac{3}{4}m + (1-m)\right)p_{Dd}(1-zh_z)(1-f)\left(1+\frac{ae}{4}\right) \tag{5d}$$

$$M_{dd} = \left(\frac{3}{4}m + (1-m)\right)\left(p_{dd} + (1-e)p_{Dd}(1-zh_z)\frac{f}{2}(1+ae)\right) \tag{5e}$$

and can be derived from the left-hand panel of Figure 1. Fitness costs can affect diploid zygotes, reducing the initial frequencies by the factors $1-z$ and $1-zh_z$ for DD and Dd genotypes, respectively. Here, h_z denotes the dominance coefficient of the costs for diploids. When monokaryons are formed, which happens with probability m, they represent $1/4$ of the nuclei in an ascus. Consequently, monokaryotic spores represent a fraction $m/4$ of the initial diploid frequencies, and dikaryons represent a fraction $\frac{3}{4}m + (1-m)$. Spore killing is affecting monokaryotic spores of the d genotype and dikaryotic spores of the dd genotype originating from Dd diploids. In these cases, killing occurs with efficiency e. Thus, a proportion $1-e$ of the sensitive spores exposed to killing survive. Importantly, monokaryotic d-spores are affected under both first- and second-division segregation, while dikaryotic spores are affected only when homoallelic (dd), and therefore only under first-division segregation (occurring with probability f). Only when the killing efficiency is maximal ($e = 1$) are all sensitive spores that are exposed to the D allele killed. In asci in which spore killing occurs, all surviving spores can benefit from a killing advantage regardless of their genotype. The killing advantage is likely to originate from additional resources made available due to some spores being killed and is therefore assumed to be proportional to the number of killed spores. For this reason, the killing advantage is weighted by the killing efficiency, providing a benefit $1 + ae$ to surviving spores. The killing advantage benefiting monokaryotic spores of an

ascus that originates from second-division segregation is special. In this case, only one nucleus per ascus can be killed in contrast to the four nuclei that are killed under first-division segregation. When this occurs, the killing advantage is $1 + \frac{ae}{4}$. Finally, $\bar{W}$ is the sum of the numerators on the right-hand side of equation (1).

2.2 The model adapted to *Podospora*

In this section, we specify the ranges for various parameters to the extent that they are known for *Podospora*. For this system, it is unknown whether spore killing alleles impose fitness costs on the carrier and if, and to what extent, a killing advantage exists. Therefore, we study the broadest possible range of fitness costs for each stage of the life cycle, from 0 (no costs) to 1 (fully lethal), and a wide range of killing advantages from 0 (no benefit) to 1 (equivalent to all killed spores being replaced). The rate of selfing in natural populations of *Podospora* is not known. However,the propensity of *Podospora* species to self in laboratory conditions, together with low overall levels of genetic diversity (Vogan et al., 2019), indicates that selfing may occur frequently; therefore, we study the effect of selfing rates ranging from 0 to 95%. Spore killers known in *Podospora* undergo first-division segregation in 30-100% of meioses, depending on the variants (van der Gaag et al., 2000; Vogan et al., 2019). We cover this range by studying the probabilities 0.25, 0.5 and 1 of first-division segregation. Under natural conditions, the occurrence of asci containing monokaryons can vary between 0% and 6% (Esser, 1974; van der Gaag, 2005). We therefore analyse the model without monokaryons first, and then with monokaryons occurring in 5% of asci to cover the natural range, and finally in 50% of asci to make the effect on spore killing dynamics more visible. Finally, the killing efficiency e is believed to be high in *Podospora* (Vogan et al., 2019). In the main part, the model is analyzed with $e = 1$ and we briefly explore incomplete killing ($e < 1$) in order to contrast its effect with that of the probability of first-division segregation $f < 1$.

2.3 The model adapted to *Neurospora*

We focus on the life cycle of heterothallic *Neurospora* species, i.e., species where different mating types occur in different individuals, such as *N. sitophila* and *N. crassa*. Since these species are sexually self-incompatible the entire population is outcrossing. We assume random mating and Hardy-Weinberg proportions, although we acknowledge that inbreeding is a possibility in *Neurospora*. Random mating greatly simplifies the model, because then the dynamics of the spore killing allele can be described by following its frequency in the pool of random mating gametes.

Thus, the dynamics in *Neurospora* can be described by following a single variable, while two variables are necessary to describe the dynamics in *P. anserina*. The dikaryotic phase of *Neurospora* is extremely short, confined to a single hypha, and therefore we do not include di- or monokaryons in the model. The vegetative stage is considered haploid. The same diploid and haploid costs z and g as in the *P. anserina*-model apply, as well as the killing efficiency e and the killing advantage a. Despite the fact that we derive the *Neurospora* model by updating D's frequency at the gamete stage, the *Neurospora* model is effectively equivalent to the *P. anserina* model with $m = 0$, $s = 0$ and $f = 1$. Figure 1 also serves as graphical illustration for the *Neurospora* life cycle when the haploid vegetative stage of *Neurospora* is considered equivalent to the dikaryotic vegetative stage of *P. anserina*.

Let p_D be the frequency of D in the gamete pool in the current generation and p'_D in the next generation. Then

$$p'_D = \frac{p_D^2 L_{DD} + p_D(1-p_D)L_D}{p_D^2 L_{DD} + 2p_D(1-p_D)(\frac{L_D}{2} + \frac{L_d}{2}) + (1-p_D)^2}, \tag{6}$$

where

$$L_{DD} = (1-z)(1-g) \tag{7a}$$

$$L_D = (1-zh_z)(1+ae)(1-g) \tag{7b}$$

$$L_d = (1-e)(1-zh_z)(1+ae). \tag{7c}$$

Here, L_{DD} represents the overall fitness costs to a D nucleus in a DD zygote, L_D to a D nucleus in a Dd zygote, and L_d to a d nucleus in a Dd zygote, which, in the last case, includes the costs of being killed.

2.4 Methods

We first analyse the deterministic recursions to characterise the parameter combinations that permit invasion and subsequent fixation of D, or invasion and subsequent stable polymorphism. To this end, we identify equilibria of the system and determine their stability. Stability is determined based on a linear stability analysis of the one-dimensional system in the case of *Neurospora* (Otto and Day, 2011, pp. 163-172) or the two-dimensional system in the case of *P. anserina* (Otto and Day, 2011, pp. 316-320). For the *Neurospora*-model we obtain analytical results that allow us to identify exact conditions for invasion and stable polymorphism as functions of the model parameters. In the case of *P. anserina*, we can only solve for equilibria and stability when parameter values are predetermined and we resort to parameter sweeps.

In order to determine the invasion probability of a spore killing allele in a finite population, we analyse a stochastic version of the model accounting for drift. To this end, the recursions define the sampling probabilities of a Wright-Fisher process, with sampling occurring at the stage of zygote formation. For each set of parameter values, the invasion probability is estimated as the proportion of 1000 simulation runs in which the spore killer achieves the equilibrium frequency of the deterministic system (fixation or stable polymorphism). A stochastic simulation is considered to have reached an internal equilibrium if allele frequencies fluctuate around the same value for at least 1000 generations. The invasion probability is taken to be zero whenever the deterministic model does not allow for invasion.

3 Results

3.1 *Podospora anserina*

3.1.1 Deterministic model

The dynamics of the spore killing allele D is affected by all parameters listed in the legend of Figure 1 and a complete analysis of all parameter combinations is out of scope. In the following, we first focus on the case of complete killing ($e = 1$) and no monokaryons ($m = 0$) and then explore the effect of e and m. Table 1 gives an overview of the investigated parameter combinations and the corresponding figures.

Table 1: **Overview of the parameter combinations investigated in the *Podospora* model.**

e	*m*	cost	dominance	Figure	
				Deterministic	Stochastic
1	0	z	h_z=0	**2**	**3**
			h_z=0.5	**S1**	**S11**
			h_z=1	**S2**	**S12**
		k	h_k=0	**S3**	**S13**
			h_k=0.5	**S4**	**S14**
			h_k=1	**S5**	**S15**
		g		**S6**	**S16**
	0.05	z	h_z=0	**S9**	-
	0.5			**S10**	-
0.8	0	z	h_z=0	**S7**	-
			h_z=0.5	**S8**	-

Generally, five outcomes are possible. (a) The killing allele cannot invade. (b) The killing

allele can invade and goes to fixation. (c) The killing allele can invade and reaches an internal equilibrium at which the killing and non-killing allele coexist in a stable polymorphism. (d) The two boundary equilibria (the frequencies 0 and 1 of the spore killer) are stable, indicating that a spore killer at low frequency would go extinct, but that it would go to fixation if starting at a sufficiently high frequency. In this case, there is an unstable equilibrium at intermediate frequency which separates the regions from where the dynamics of the killing allele either approach extinction or fixation. (f) The killing allele can invade and there are two internal equilibria, with the lower one stable and the higher one unstable. This last case is rare.

(i) Effects of different fitness costs with $e = 1$ and $m = 0$. Figure 2 shows the number, location and stability properties of the equilibria as a function of the recessive diploid costs z, the killing advantage a, the selfing rate s and the probability of first-division segregation f. The possibility for a spore killer to invade is determined by an interaction of all parameters, with high values of a and f favoring invasion and high values of s and z disfavoring it. Invasion becomes more difficult with increasing dominance of the fitness costs z (compare Figure 2 with S1 and S2). When fitness costs are dominant, they affect the dynamics of the spore killer in a very similar way regardless of the stage of the life cycle at which they occur (diploid, dikaryotic or haploid; compare Figures S2, S5 and S6). In contrast, when dikaryotic and diploid costs are additive or fully recessive, costs at the diploid stage have less of a negative effect on the invasion of the D-allele than costs at the dikaryotic stage (compare Figure 2 with S3 and S1 with S4). This difference is magnified with increasing probability of first-division segregation f and can be explained by the fact that diploid costs are independent of spore killing events as they occur before meiosis, while dikaryotic costs occur at the same stage as spore killing. For this reason, recessive or additive diploid costs affect the spore killer very little at the onset of invasion when homozygote DD individuals are rare, and the costs in heterozygotes are shared between the D and d alleles. On the other hand, dikaryotic costs are linked to spore killing through the probability of first-division segregation during meiosis. First-division segregation is necessary for killing to occur, but it also generates homoallelic dikaryons DD which suffer from high costs.

In this first scenario based on $e = 1$ and $m = 0$, coexistence between the spore killer and the non-killing allele is only possible with recessive fitness costs to the killer (Figure 2 and supplementary Figure S3). These costs need to be compensated for by a killing advantage to allow for invasion in the case of dikaryotic costs, but this is not necessary for diploid costs with selfing rate $s = 0$, because, as explained in the previous paragraph, diploid costs affect spore killers very little during early invasion.

In addition to costs and killing advantage, the probability of first-division segregation f and

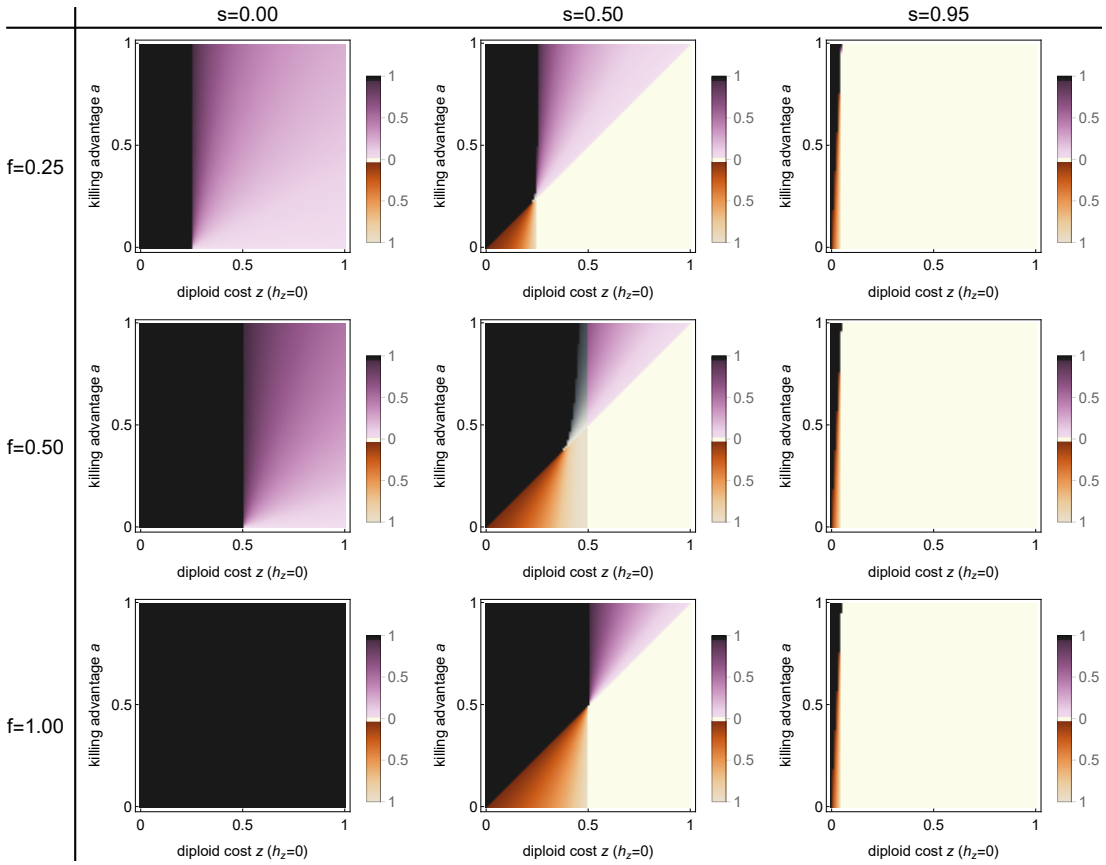

Figure 2: **Bifurcation analysis of the *Podospora* model with recessive ($h_z = 0$) diploid fitness costs** z. Diploid fitness costs z, killing advantage a, selfing rate s and probability of first-division segregation f are bifurcation parameters. Extinction ($\hat{p}_D = 0$) and fixation ($\hat{p}_D = 1$) of the killer allele D always constitute equilibria. Additionally, one or two interior equilibria at intermediate frequencies are possible. Parameter regions are color coded as follows: **white**, D cannot invade and $\hat{p}_D = 0$ is a globally stable equilibrium; **black**, D can invade and reach fixation, $\hat{p}_D = 1$ is a globally stable equilibrium; **purple**, D can invade but cannot reach fixation and coexists with the non-killing allele d at a globally stable interior equilibrium $0 < \hat{p}_D < 1$, whose value is given by the shade of purple; **brown**, the two boundary equilibria $\hat{p}_D = 0$ and $\hat{p}_D = 1$ are stable and separated by an unstable interior equilibrium $0 < \hat{p}_D < 1$, whose value is given by the shade of brown; **gray**, two interior equilibria exist, the equilibrium with the lower value is stable, meaning that D can invade and coexist with d at a stable interior equilibrium, whose value is given by the shade of gray. Each panel is based on 100x100 parameter combinations. Other fixed parameters: $e = 1$, $m = 0$, other fitness costs to zero.

the selfing rate s interact, with f favoring the fixation of the spore killer and s preventing its invasion. The effect of f is present when s is small but becomes negligible when s is high. This interaction occurs because killing efficiency only matters as long as the population of heterozygotes is not a limiting factor for killing. New heterozygotes can only be produced through outcrossing, so a high selfing rate becomes the limiting factor for the rate of killing itself.

(ii) Effect of e with recessive and additive diploid fitness costs z. Next, we explore the roles of the killing efficiency e. We restrict ourselves to the case of diploid costs, which is the case most conducive to invasion of the killing allele. Figure S7 shows a bifurcation diagram analogous to Figure 2 but with $e = 0.8$. Two observations can be made when comparing these two figures. First, lowering the killing efficiency from $e = 1$ to $e = 0.8$ reduces the maximum value of z for the diploid costs that allows for the invasion of allele D, in particular, when the killing advantage a is high. This is expected because the driving action of the spore killer is reduced. Second, the minimum value of z for the diploid costs that allows a population fixed for the killing allele D to be invaded by the sensitive allele d decreases. When costs are recessive, this shifts the boundary between the parameter region corresponding to fixation and the region corresponding to coexistence to lower values of z, and, in the absence of selfing ($s = 0$), increases the parameter region allowing for coexistence. Both these observations also apply under additive costs (compare Figures S1 and S8). Interestingly, in the latter case coexistence is not possible under complete killing ($e = 1$, Figure S1) but a parameter region allowing for coexistence appears with reduced killing efficiency ($e = 0.8$, Figure S8). To explain the second observation, we need to highlight an important distinction between the probability of first-division segregation f and killing efficiency e. Although both contribute to the spore killer's rate of killing, f determines the frequency of meiosis events resulting in asci where killing occurs, while e determines the efficiency of killing once the killing and sensitive alleles already share the same ascus. It follows that a reduced killing efficiency ($e < 1$) allows sensitive spores to survive a killing event, while a reduced probability of first-division segregation ($f < 1$) simply avoids sensitive spores being exposed to the killer. A killing advantage a benefits all spores that survive a killing event, regardless of their genotype. Thus, incomplete killing ($e < 1$) provides surviving sensitive spores with a killing advantage, which causes the fixation equilibrium to become unstable.

(iii) Effect of m with recessive diploid fitness costs z. A final aspect of the *P. anserina* life cycle that we explore is the effect of monokaryons on the dynamics of the spore killer. As can be seen from the life cycle in Figure 1, the occurrence of monokaryons allows for a small amount of spore killing even in the case of second-division segregation, and that monokaryons are not able to self. As a result, monokaryons could favor spore killing by limiting the effective selfing rate, and by

allowing killing even when the probability of first-division segregation is low. When monokaryons occur in an ascus resulting from second-division segregation, incomplete killing ensues and we expect dynamics similar to the case of incomplete killing efficiency ($e < 1$) discussed above.

Following the life cycle in Figure 1, we can express the proportion K of spores that are killed during meiosis as

$$K = P_{Dd} e(1 - zh_z) \left(\frac{f}{2} + \frac{m(1-f)}{4 \times 2} \right). \tag{8}$$

Thus, the number of killed spores increases with the proportion of monokaryons m and of course with the frequency P_{Dd} of heterozygote individuals in the population, which is also favored by m. In the supplementary Figures S9 and S10, we show how monokaryons affect the dynamics of spore killing for the case of recessive diploid fitness costs, with 5% and 50% of asci containing a pair of monokaryons, respectively. A frequency of 5% is in the range expected in natural populations, while 50% is presented to magnify the effect and make it more appreciable. These figures should be compared to Figure 2, which shows the same dynamics without monokaryons. In the case of 50% of asci containing monokaryons, the expected effects of monokaryons become clearly visible (see Figure S10). We observe a reduction of the negative impact of selfing on spore killer invasion, and a larger space for coexistence, due to incomplete killing similar to the case $e < 1$. With 5% of asci containing monokaryons, the impact of monokaryons appears negligible, indicating that they may not matter to spore killer dynamics under natural conditions.

Somewhat simplified, the results for the *Podospora* model can be summarized as follows. A spore killer can invade if it bears no fitness costs, or if the costs are out-weighed by the fitness benefit due to a killing advantage. Selfing magnifies the effect of costs, and reduces the frequency of heterozygote individuals necessary for spore killing. Selfing interacts with the probability of first-division segregation to determine the effective killing rate. Coexistence between a spore killer and a sensitive allele is possible if (i) the killing efficiency is perfect ($e = 1$) in combination with recessive fitness costs and either some amount of selfing or second-division segregation during meiosis, or (ii) with incomplete killing efficiency ($e < 1$) in combination with recessive or additive fitness costs.

3.1.2 Invasion probability

Our stochastic simulations confirm that invasion of the killing allele D is possible whenever the equilibrium $\hat{p}_D = 0$ is unstable. The probability of invasion increases with the probability of first-division segregation f and the killing advantage a, which both contribute to a selective advantage of the spore killer. In turn, invasion probability decreases with fitness costs (e.g. diploid costs z in

Figure 3) and the selfing rate s. The results for other fitness costs are presented in supplementary Figures—we refer the reader to Table 1 for an overview of the parameter combinations investigated and the corresponding figures. We find that when the spore killer is associated with a killing advantage or fitness costs or both the dependency of the invasion probability on population size becomes negligible (see supplementary Figure S17). We refer the reader to Box 2 later in this section for our analysis of the dependency of invasion probability on population size for the case that a killing advantage and fitness costs are absent.

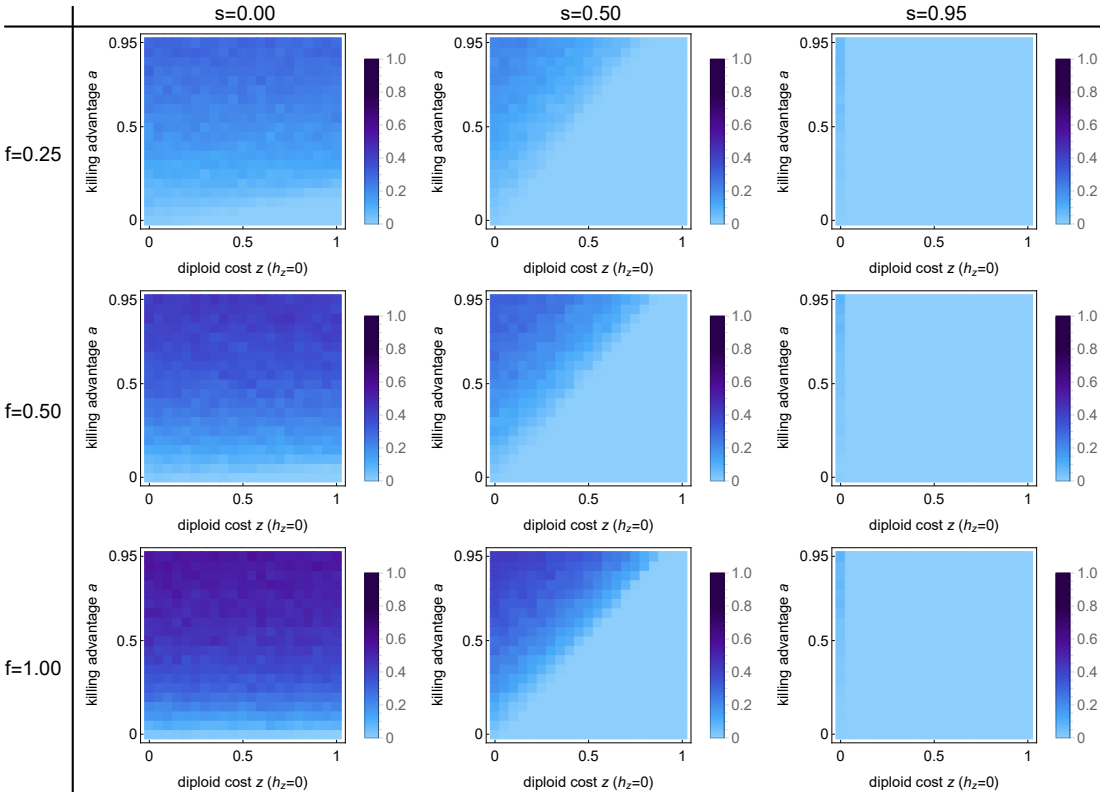

Figure 3: **Invasion probability of a spore killing allele D for the *Podospora* model with recessive $(h_z = 0)$ diploid fitness costs z.** Parameters are the fitness costs z, the killing advantage a, the selfing rate s and the probability of first-division segregation f. Each panel consists of 21x21 parameter combinations and shades of blue indicates the invasion probability estimated from 10^3 stochastic Wright-Fisher simulation runs with a population size of 1000. Other parameters as in Figure 2.

Box 2. Invasion probability of a spore killer without killing advantage.

A spore killer without killing advantage is a relative drive and consequently its invasion probability tends to zero as population size N becomes large. However, it has not been demonstrated how rapidly this invasion probability declines as N grows, and how the effects of population size on invasion probability and mutational supply interact to determine the rate of invasion of spore killers.

Invasion probability as a function of population size N.

We study the simplest possible model of a newly-arisen spore killer with 100% killing efficiency, assuming random mating (including no selfing). Employing a heuristic method from Desai and Fisher (2007, p.1763), we show in **Appendix 2** that, once the spore killer exceeds $n = \sqrt{N}$ copies, the expected increase in its copy number over the subsequent n generations ($\sim n^3/N$) is greater than typical decreases in copy number by random drift over the same period ($\sim n$), so that the spore killer has very likely escaped stochastic loss. The dynamics of the spore killer before reaching $\sqrt{N}$ copies are dominated by random drift, so the probability that it attains the required $\sqrt{N}$ copies — i.e., its invasion probability — is approximately: $\sqrt{N}/N = \mathbf{1}/\sqrt{\boldsymbol{N}}$. This approximation accords well with estimates obtained from simulations (see panel (a)).

Invasion rate as a function of population size N.

If spore killers arise at a rate μ per replication, then their rate of appearance per generation is $N\mu$. Therefore, the per-generation rate of invasion of such spore killers is $N\mu \times 1/\sqrt{N} = \sqrt{\boldsymbol{N}}\boldsymbol{\mu}$. The invasion rate is therefore an increasing function of population size (see panel (b)), despite the fact that the invasion probability of each individual spore killer decreases, and indeed tends to zero in the large-population limit. Additional life-history features, such as selfing affect the invasion rate but do not affect the positive scaling with population size (panel (b)).

Invasion probability and population structure.

The dependence of the invasion probability on N suggests that population structure could significantly affect the rate at which spore killers invade. Suppose that a population of size N is subdivided into M demes, each of size $m = N/M$. The overall arrival rate of new spore killers is unchanged ($N\mu$) but, since invasion of one deme guarantees population-wide invasion (unless m is very small), the invasion probability is $1/\sqrt{m}$. The invasion rate is therefore $N\mu \times 1/\sqrt{m} = \mu\sqrt{m}\sqrt{N}$, which is larger than in an unstructured population by a factor $\sqrt{\boldsymbol{M}}$. A similar result has been obtained for recessive beneficial mutations, which are under similar frequency-dependent selection (Gale 1990, p.180-181).

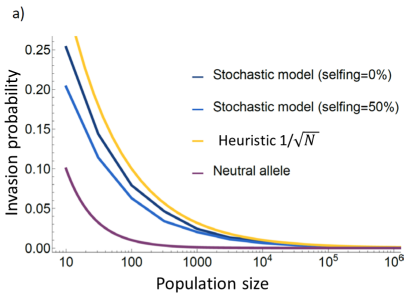

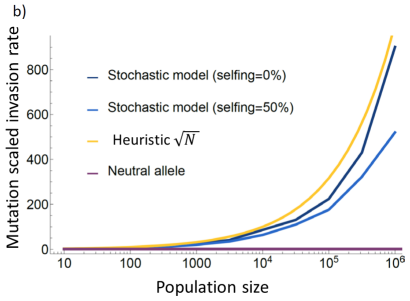

Take-home

Even spore killers without killing advantage can exhibit an appreciably large invasion probability. They are expected to invade at a non-negligible rate, especially in large, fragmented populations, unless their appearance by mutation is extremely infrequent.

3.2 *Neurospora*

3.2.1 Deterministic model

The dynamics of the spore killing allele D in *Neurospora*, as described by Equation (6), can be analyzed analytically. Solving this equation for its equilibria, we obtain $\hat{p}_D = 0$, $\hat{p}_D = 1$ and

$$\hat{p}_D = \frac{1 - L_D}{1 - L_D + L_{DD} - L_d}. \tag{9}$$

The last solution is a valid equilibrium (i.e., $0 < p_D < 1$) if $L_D < 1$ and $L_{DD} > L_d$, or if $L_D > 1$ and $L_{DD} < L_d$. A linear stability analysis shows that the killing allele D can invade ($\hat{p}_D = 0$ unstable) if $L_D > 1$. This condition makes intuitive sense, as it means that the spore killing allele D can invade when its fitness in a heterozygote is higher than that of the sensitive resident allele d in a homozygote, taking into account potential fitness costs and killing advantage. More specifically, from equation (7b) we can see that the necessary condition for invasion is that the realised killing advantage ae (killing advantage times killing efficiency) outweighs the decrease in fitness in heterozygotes, due to g and zh_z. In addition, in the special case where $L_D = 1$, a linear stability analysis shows that the spore killer can still invade as long as $e > 0$. This scenario can occur if there are not cost and no killing advantage associated to the spore killer or if the two parameters compensate each other. The spore killer reaches fixation when the fitness of D in a homozygote is higher than that of d in a heterozygote, $L_{DD} > L_d$. This means that a sensitive allele d is unable to invade a population in which the killing allele D is fixed. Based on equations (7a) and (7c), this is the case when the reduction of homozygous fitness due to z or g is less than the combined effect of killing efficiency e, heterozygous costs zh_z and realised killing advantage ae on the fitness of the sensitive allele d in heterozygotes.

The two conditions for invasion and fixation lead to four possible scenarios. First, if $L_D \geq 1$ and $L_{DD} > L_d$, the spore killer can invade and reach fixation: $\hat{p}_D = 1$ is a globally stable equilibrium. Second, if $L_D < 1$ and $L_{DD} < L_d$, the spore killer cannot invade and $\hat{p}_D = 0$ is a globally stable equilibrium. Third, if $L_D \geq 1$ and $L_{DD} < L_d$, the spore killer can invade and coexist with the sensitive allele at a stable polymorphism. Fourth, if $L_D < 1$ and $L_{DD} > L_d$, the spore killer cannot invade from low frequencies, but it can reach fixation if starting from a frequency higher than that given by equation (9).

We can now identify the following conditions necessary for stable coexistence. First, killing has to be incomplete ($e < 1$), as otherwise $L_d = 0$. Second, with $e < 1$ fitness costs have to exist ($z > 0$ or $g > 0$), since the condition $L_{DD} < L_d$ would otherwise require that $a > 1$, which is biologically not feasible. Third, in the absence of a killing advantage ($a = 0$) fitness costs have to be recessive (implying a diploid cost with $h_z = 0$ and no haploid cost $g = 0$) for the spore killer to be able to invade, and diploid fitness costs to exceed the killing efficiency ($z > e$) to prevent fixation of the killer.

Figure 4 shows how the equilibria are affected by the killing efficiency e, the killing advantage a, the diploid cost z and its degree of dominance h_z (similar results for the case of haploid costs are shown in the Supplementary Figure S18). Generally, the parameter space for coexistence becomes larger with fitness costs being more recessive and lower killing efficiency.

It is worth highlighting a phenomenon that is specific to spore killing and relies on a killing advantage. Since a killing advantage results from additional resources to spores that survive killing, it also benefits spores that do not carry D but survive killing, provided $e < 1$. This mechanism creates a region for coexistence in parameter space that does not require the fitness costs to the spore killer to be recessive (purple regions in the second column in Figure 4). This coexistence is made possible by the killing advantage, which prevents fixation of the spore killer in a similar way to the recessive costs of a killing allele.

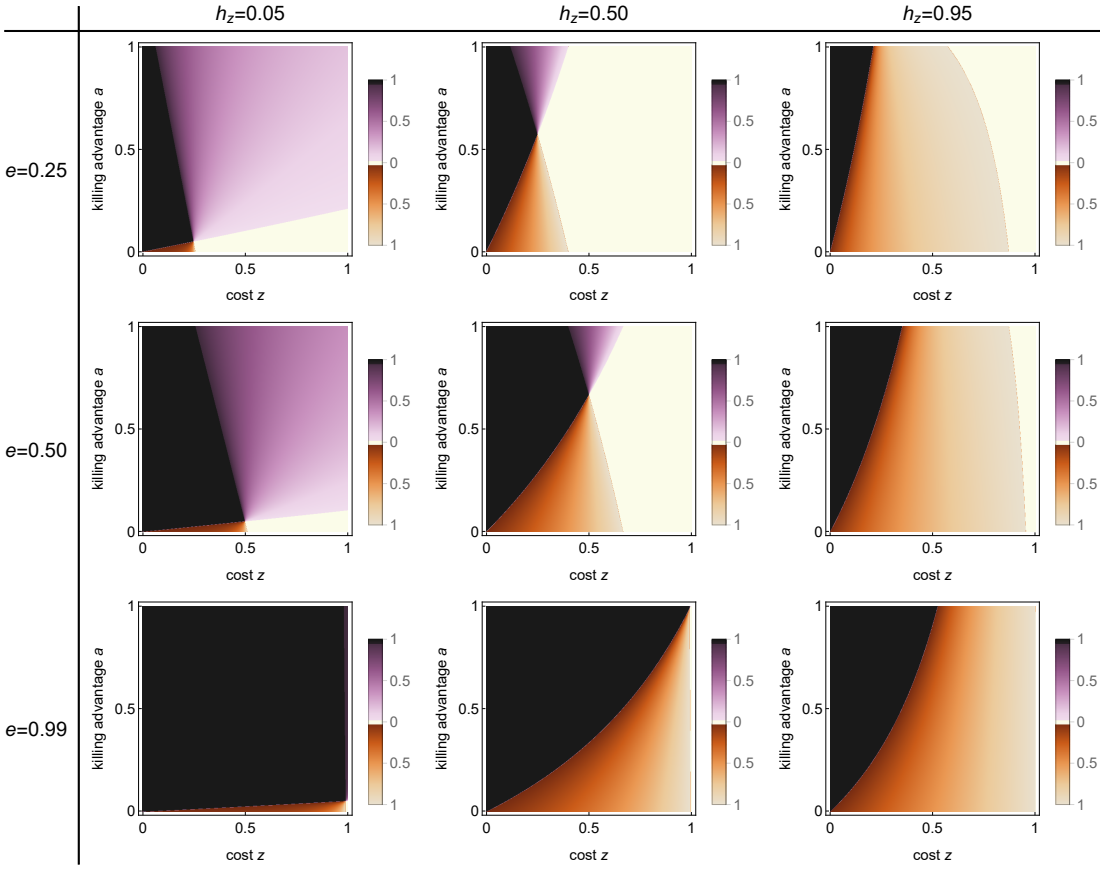

Figure 4: **Bifurcation analysis of the *Neurospora* model with diploid fitness costs** z. Diploid fitness costs z and their dominance parameter h_z, killing advantage a, and killing efficiency e are bifurcation parameters. Extinction ($\hat{p}_D = 0$) and fixation ($\hat{p}_D = 1$) of the killer allele D always constitute equilibria. Additionally, one interior equilibrium is possible. Parameter regions are color coded as follows: **white**, D cannot invade and $\hat{p}_D = 0$ is a globally stable equilibrium; **black**, D can invade and reach fixation, $\hat{p}_D = 1$ is a globally stable equilibrium; **purple**, D can invade but cannot reach fixation, instead it coexists with the non-killing allele d at a globally stable interior equilibrium $0 < \hat{p}_D < 1$, whose value is given by the shade of purple; **brown**, the two boundary equilibria $\hat{p}_D = 0$ and $\hat{p}_D = 1$ are stable and separated by an unstable interior equilibrium $0 < \hat{p}_D < 1$, whose value is given by the shade of brown. Each panel is based on 1000x1000 parameter combinations. Fitness costs $g = 0$.

Somewhat simplified, the results for the *Neurospora* model can be summarized as follows. A spore killer can invade if it bears no fitness costs, or if the costs in heterozygote individuals are out-

weighed by the fitness benefit due to a killing advantage. If the killer allele can invade, then stable coexistence with the sensitive allele is possible provided that (i) killing is incomplete ($e < 1$) and (ii) there are either sufficiently strong fitness costs to the spore killer when homozygous (recessive fitness costs) or a strong killing advantage that benefiting the sensitive allele.

3.2.2 Invasion probability

As in the case of *Podospora*, our stochastic simulations show that, for the *Neurospora* model, invasion of the killing allele D is possible whenever the equilibrium $\hat{p}_D = 0$ is unstable. The probability of invasion increases with decreasing costs and decreasing dominance of the costs, increasing killing advantage and increasing killing efficiency (Figures S20 and S19).

4 Discussion

We explore the effect of several aspects of fungal life cycles on the conditions under which a spore killing allele can invade and subsequently stably coexist with a non-killing allele. In ascomycete fungi, spore killing takes place within the ascus, and our model is based on a detailed mechanistic understanding of ascus composition (see Figure 1). Our results show that following the different possible compositions of spores within an ascus is necessary for a detailed understanding of the dynamics of a spore killing allele. Another novel aspect of our study is the development of stochastic models to investigate the invasion probability of a spore killing allele, which complements our deterministic analysis. Our model is based on a single allele responsible for both spore killing and resistance to spore killing. Thus, there is no recombination between the two functions. This feature is consistent with the picture emerging from recent genetic characterization of spore killers in several species of ascomycete fungi (Nuckolls et al., 2017; Hu et al., 2017; Vogan et al., 2019; Svedberg et al., 2020). The only other theoretical study of spore killing known to us (Nauta and Hoekstra, 1993) focused on the role of recombination between the killing and resistance functions, which was appropriate given what was known about the genetic architecture of spore killers at that time in *Neurospora*, but appears now to be the exception rather than the rule.

In the following, we first discuss the general insights that our model reveals about the invasion of spore killers. We then discuss our results in the light of data from natural systems, with particular attention paid to the spore killer systems *Spk-1* in *Neurospora* and *Spok* in *Podopsora* (which inspired our model). Throughout, we contextualize our findings with respect to theoretical and empirical results from male and female meiotic drivers in animals and plants.

4.1 Spore killers in theory

4.1.1 Selective advantage and invasion of a spore killer

We start by comparing the dynamics of spore killers in our model with Hartl's 1972 general model of sperm and pollen killers. In Hartl's model, gamete killers kill in the homozygote form, which could be seen as "self-killing" or "suicide" as effectively the killer allele eliminates other copies of itself. This "self-killing" does not provide any fitness advantage for the killer in the absence of a killing advantage. In contrast, spore killers do not "self-kill", which allows them to obtain a positively frequency-dependent selective advantage simply by killing. In agreement with Nauta and Hoekstra (1993), we find that this frequency-dependent selective advantage tends to zero when the frequency of the spore killer is close to zero, for example, when invading a very large population. In the absence of any killing advantage, the selective advantage of a spore killer is thus minimal at the onset of invasion, and smaller the larger the population that is to be invaded. Spore killers may therefore not be able to invade if any non-recessive fitness costs are associated with them, or simply in very large populations because the chances of stochastic loss early in the invasion are very high (see Box 2). This feature clearly distinguishes spore killers from female drive systems (e.g. Hall and Dawe, 2018), in which the selective advantage due to meiotic drive alone may be sufficient to compensate for substantial fitness costs.

Although the invasion probability of a spore killer without killing advantage is substantially lower than that of a female driver, it is not negligible (Box 2). Moreover, owing to the frequency-dependent nature of the spore killer's selective advantage, small or fragmented populations may represent easier targets for invasion; thus, the study of spore killers in structured populations, which we have only briefly addressed in Box 2, could represent an interesting prospect for future theoretical studies. In addition, we suggest that the invasion rate of spore killers could in fact increase with population size, even in the absence of killing advantage, as the inflation of the mutational supply of spore killers more than compensates for the decrease in the invasion probability of each individual spore killer (Box 2). This last point is, of course, dependent on the mechanism of origin of spore killers, which we discuss in the next section.

In addition to the killing itself, we propose that spore killers could obtain a killing advantage, i.e., a net fitness benefit from killing, either in the form of compensation or reduced local competition for resources. In the model of Hartl (1972), compensation plays a crucial role for gamete killers, as it grants them a selective advantage. Although we cannot draw a direct parallel since Hartl's model focuses on the role of fecundity functions, we also find that a killing advantage is crucial for the invasion of a spore killer since it does not rely on the killing allele to be sufficiently

frequent, and benefits the spore killer even during the early phase of invasion. In particular, a killing advantage reduces the chance of stochastic loss of a killing allele. It is therefore important for future empirical explorations to determine whether and to what extent a killing advantage is present in order to better understand spore killer dynamics.

4.1.2 Coexistence of a spore killing allele with a non-killing allele

We also investigate the conditions for coexistence of the killing and non-killing alleles. Meiotic drivers (MDs) are often expected to spread to fixation rapidly (Lindholm et al., 2016) instead of coexisting with their non-driver alleles in a stable polymorphisms, and when a MD is fixed it becomes undetectable. The MDs that are observed in natural conditions are therefore expected to exhibit (possibly unusual) properties that allow them to be maintained in a stable polymorphism. Understanding these properties is thus an important part of theoretical studies of meiotic drive. Classically, in male and female drive, recessive fitness costs associated with the driving allele are required for coexistence (e.g., Hartl, 1970; Fishman and Kelly, 2015; Lewontin and Dunn, 1960; Holman et al., 2015). Coexistence can then occur because the costs are expressed in the homozygote form, preventing fixation, but not in the heterozygote form, permitting invasion. We find this dynamics in our models for both *Neurospora* and *Podospora*. Fitness costs are needed for coexistence to be possible and recessive costs increase the parameter space allowing for coexistence, as seen in Figure 2. For coexistence to be possible, it is also necessary for killing not to be complete, so that the sensitive allele has a positive fitness when in a diploid heterozygote. Incomplete killing can result from the killing efficiency being less than 100%, and, in the case of *Podospora*, from second-division segregation.

We also find that coexistence is possible even if fitness costs to the spore killer are not recessive. Such coexistence occurs because sensitive spores that survive killing also benefit from the killing advantage. We believe that this assumption is reasonable given the two possible scenarios that we envision can cause a killing advantage, namely compensation and reduction in local competition. Compensation results in additional spores—both killer and sensitive—being produced by the parent. If a killing advantage occurs through a reduction in local competition with siblings, then the same reasoning applies and both types of surviving spores obtain a fitness advantage. Coexistence can occur in that case because the benefit to the surviving sensitive spores prevents fixation of the spore killer by raising the fitness of the sensitive allele in the heterozygote form above the fitness of the homozygote spore killer. Thus, incomplete killing can result in coexistence just as recessive costs can (or overdominance, Hartl, 1970), but the underlying biology is distinct.

4.1.3 Mating system and spore killer dynamics

We find that the rate of selfing of the host has a negative effect on the invasion of a spore killer. The reason is that selfing decreases the frequency of heterozygotes necessary for spore killing to occur, and magnifies potential fitness costs by generally slowing down invasion. Because of this latter point, our model predicts that a spore killer is able to invade a population with a high selfing rate only when associated with very low fitness costs, and that coexistence is then unlikely. We expect inbreeding to have the same effect as selfing, and analyzing spore killer models in which the assumption of random mating is relaxed could be an interesting next step. The effect of selfing also suggests that mating behavior itself, either through selfing or inbreeding, could evolve as a defence mechanism against spore killers, as suggested by Lewontin and Dunn (1960). Along the same lines, Bull (2017) and Bull et al. (2019) have developed models showing that inbreeding could evolve as an efficient response to costly meiotic drivers. Their results can also be linked to the model of Burt and Trivers (1998), which suggests, with empirical support, that obligatory outcrossing plant species are more susceptible to costly selfish genetic elements.

4.2 Insights from natural systems

4.2.1 How much do we know about spore killers in nature?

In several model systems of male and female drive, the molecular mechanism of the MD, its fitness effects and the biology of the host are known to a sufficient extent that population genetics models can predict the frequency of the MD in natural or laboratory populations with impressive accuracy (e.g. Fishman and Kelly, 2015; Lewontin and Dunn, 1960). In the case of spore killers, however, although several recent publications shed light on the genetic and molecular basis of their driving action (Vogan et al., 2019; Svedberg et al., 2020; Nuckolls et al., 2017; Hu et al., 2017), many unknowns remain, particularly regarding the ecology of the hosts. This makes accurate predictions difficult. In this section, we summarize the available knowledge and use it to put our results in perspective and to suggest future directions for empirical research.

We focus on the three spore killers in fungal hosts that are best understood: the *Spok* gene family in *Podospora anserina* (Vogan et al., 2019) and *Spk-1* in *Neurospora sitophila* (Svedberg et al., 2020), both of which directly inspired our models, and finally the *wtf* gene family in *Schizosaccharomyces pombe* (Hu et al., 2017; Nuckolls et al., 2017), which is also well studied and has many similarities with the first two. In all three cases, spore killing and resistance are governed by a single locus, which matches the assumption about the genetic architecture in our model.

Little is known about the origin of spore killers. It has been proposed that spore killing systems may arise neutrally in populations in which resistance to killing has been fixed first (Sweigart et al., 2019). According to this view, spore killers would act as a strong type of hybrid incompatibility evolved between diverging populations. However, our work shows that an active spore killer has a greater chance of invading than a neutral allele, which suggests that selfish evolution of spore killers is more likely. The *Spok*s, *Spk-1* and *wtf*s all belong to large families of genes that occur across complexes of closely related fungal taxa. This observation suggests the possibility of horizontal gene transfer across species. For example, there is evidence that *Spk-1* in *N. sitophila* may have introgressed from the closely related *N. hispaniola* (Svedberg et al., 2020). In addition to their apparently frequent movements, *Spok* and *wtf* genes mutate rapidly (Vogan et al., 2019; Nuckolls et al., 2017; Hu et al., 2017), which could be the key to their success (see Box 2 for the importance of mutation rate).

4.2.2 Insights from our models on spore killer dynamics in natural populations

The *Spok* gene family has several members present in the genomes of species from the *Podospora* genus. In *P. anserina* in particular, three genes are known, *Spok2*, *Spok3*, and *Spok4*. Any given individual of *P. anserina* might carry none, one, two or all three *Spok* genes. More than one copy of a *Spok* gene might occur in a single genome, but this seems to be very rare. *Spok3* and *Spok4* occur in a genomic region known as the '*Spok* block' (Vogan et al., 2019). The different *Spok* genes act independently; that is, carrying one of them does not protect against another one (Grognet et al., 2014; Vogan et al., 2019). Supplementary Figure S21 shows the frequency of the three *Spok* genes in samples from a population of *P. anserina* near Wageningen in the Netherlands over a 17 year period. None of the spore killers reached fixation or went extinct during this period. However, *Spok2* appears close to fixation while *Spok3* and *Spok4* occur at lower frequencies. Additionally, all individuals without *Spok2* seem to derive from a single deletion, thus, *Spok2* may have been fixed prior to 1993. This is surprising given the fact that *Spok4* kills with 100% efficiency while *Spok2* does not (Vogan et al., 2019). Instead, the explanation could be that the genes *Spok3* and *Spok4* co-occur in the '*Spok* block' (Vogan et al., 2019), which is known to impose fitness costs on its host (Vogan et al., 2020). The costs associated with the'*Spok* block' get magnified due to the high selfing rate found in *P. anserina* (van der Gaag, 2005). Indeed our model predicts that selfing combined with fitness costs severely reduces the scope for invasion of a spore killer (e.g. figure S16), while the effect of killing efficiency in combination with high selfing rates on the invasion potential of spore killers is minor (compare the second and third column in figures 2 and S7).

The gene *Spk-1* in *N. sitophila* shows variation across populations, being respectively fixed

and absent in two clades that coexist in sympatry and polymorphic in a third clade, where a form of resistance to the killer has evolved (Svedberg et al., 2020). This data suggests that the dynamics of the same spore killer may follow very different routes in different populations. In the polymorphic clade, resistance had evolved in the form of reduced killing efficiency, leading to what appears to be coexistence (Svedberg et al., 2020).

Very little is known about the frequency of the *wtf*-allele in natural populations of *S. pombe* and we can only speculate from the little information that we have. Killing efficiency is lower than 100% (Nuckolls et al., 2017; Núñez et al., 2020) and selfing is likely common in *S. pombe* (Tusso et al., 2019; Nieuwenhuis and James, 2016). Furthermore, *S. pombe* is able to perform haploid selfing, a feature that is not found in *P. anserina* and that we therefore did not incorporate in our model. Based on this information, we predict that the fitness costs of *wtf* must be low to allow for invasion, that invading spore killers progress slowly and are sensitive to stochastic loss.

At least one supressor counteracting the action of the spore killer has evolved in *S. pombe* (Nuckolls et al., 2017; Núñez et al., 2020). Suppressor genes are likely to evolve if given enough time (slow invasion or stable coexistence) and are found in many other drive systems, but not in *P. anserina* so far (Vogan et al., 2019).

The spore killers *Spk-1*, *Spok* and *wtf* are all small genomic regions without inversions, suggesting that they are not necessarily associated with hitchhiking deleterious mutations (but see Vogan et al., 2020). At the same time, all spore killers function with a poison-antidote mechanism targeting spores, and it is easy to envision direct fitness costs of exposing spores to a toxin. These costs could be recessive if subject to a threshold dosage effect. As to date, there is no definitive evidence for or against fitness costs of carrying these spore killers, except for *Spok3* and *Spok4*, which are contained within the '*Spok* block' element. In that last case, it is not clear whether the cost originates from the *Spok* genes themselves or other features of the block. Finally, there is evidence from laboratory studies for a killing advantage in *P. anserina* (Vogan et al., 2020) but more work remains to be done to understand its importance in a natural setting.

4.3 Conclusions

Despite their particularities, we predict that spore killers should show similarities with well-studied systems of meiotic drive. We expect, for example, fitness costs, likely but not necessarily recessive, to explain coexistence. Like other meiotic drivers, spore killers may as well play a role in population divergence as empirical data suggests for both *wtf* and *Spk-1*. Our study identifies characteristics of the ecology and the life cycle of ascomycete fungi that are of importance for the dynamics

of spore killers. These are: fitness costs, killing advantage, host population size and the mating system. Although we find that a spore killer without costs or killing advantage is substantially more likely to invade than a neutral allele, killing advantage makes invasion much more likely still. In contrast, selfing of the host and fitness costs associated with the killer can impede its invasion or stop its spread at intermediate frequencies.

With this work, we have explored the dynamics of spore killers in two species of ascomycete fungi, and revealed novel aspects of their dynamics. We have also come to realise that many unknowns remain from both theoretical and empirical angles before we can understand and predict spore killer dynamics well. With the advent of artificial meiotic drive, a new world of possibilities opens for biological control (Esvelt et al., 2014). If spore killers are to be used for the control of fungal pest species, there is still much work that needs to be done in order fully account for their dynamics. We suggest several points of focus for future research. Important empirical tasks will be to better understand the ecology of fungal host, in particular regarding their mating systems, as well as to characterize better interactions between spore killers and their hosts (fitness effects, killing advantage). From a theoretical perspective, we suggest that the role of population structure and the possibility for the evolution of suppressor genes in spore killers should be important aspects.

References

Akbari, O. S., K. D. Matzen, J. M. Marshall, H. Huang, C. M. Ward, and B. A. Hay. 2013. A synthetic gene drive system for local, reversible modification and suppression of insect populations. Current Biology 23:671–677.

Brand, C. L., A. M. Larracuente, and D. C. Presgraves. 2015. Origin, evolution, and population genetics of the selfish *Segregation Distorter* gene duplication in European and African populations of *Drosophila melanogaster*. Evolution 69:1271–1283.

Buckler, E. S., T. L. Phelps-Durr, C. S. K. Buckler, R. K. Dawe, J. F. Doebley, and T. P. Holtsford. 1999. Meiotic drive of chromosomal knobs reshaped the maize genome. Genetics 153:415–426.

Bull, J. J. 2017. Lethal gene drive selects inbreeding. Evolution, Medicine, and Public Health 2017:1–16.

Bull, J. J., C. H. Remien, and S. M. Krone. 2019. Gene-drive-mediated extinction is thwarted by population structure and evolution of sib mating. Evolution, Medicine, and Public Health 2019:66–81.

Burt, A., and R. Trivers. 1998. Selfish DNA and breeding system in flowering plants. Proceedings of the Royal Society of London. Series B: Biological Sciences 265:141–146.

———. 2009. Genes in conflict: the biology of selfish genetic elements. Harvard University Press, Cambridge.

Crow, J. F. 1991. Why is Mendelian segregation so exact? BioEssays 13:305–312.

Desai, M. M., and D. S. Fisher. 2007. Beneficial mutation–selection balance and the effect of linkage on positive selection. Genetics 176:1759–1798.

Didion, J. P., A. P. Morgan, A. M.-F. Clayshulte, R. C. Mcmullan, L. Yadgary, P. M. Petkov, T. A. Bell, D. M. Gatti, J. J. Crowley, K. Hua, et al. 2015. A multi-megabase copy number gain causes maternal transmission ratio distortion on mouse chromosome 2. PLoS Genetics 11:e1004850.

Esser, K. 1974. *Podospora anserina*. Pages 531–551 *in* Bacteria, Bacteriophages, and Fungi. Springer.

Esvelt, K. M., A. L. Smidler, F. Catteruccia, and G. M. Church. 2014. Emerging technology: concerning RNA-guided gene drives for the alteration of wild populations. Elife 3:e03401.

703 Fishman, L., and J. K. Kelly. 2015. Centromere-associated meiotic drive and female fitness vari-
704 ation in *Mimulus*. Evolution 69:1208–1218.

705 Fishman, L., and A. Saunders. 2008. Centromere-associated female meiotic drive entails male
706 fitness costs in monkeyflowers. Science 322:1559–1562.

707 Frank, S. A. 1991. Divergence of meiotic drive-suppression systems as an explanation for sex-biased
708 hybrid sterility and inviability. Evolution 45:262–267.

709 Gale, J. S. 1990. Theoretical Population Genetics. Unwin Hyman, London.

710 Grognet, P., H. Lalucque, F. Malagnac, and P. Silar. 2014. Genes that bias Mendelian segregation.
711 PLoS Genetics 10:e1004387.

712 Haig, D., and C. T. Bergstrom. 1995. Multiple mating, sperm competition and meiotic drive.
713 Journal of Evolutionary Biology 8:265–282.

714 Hall, D. W., and R. K. Dawe. 2018. Modeling the evolution of female meiotic drive in maize. G3:
715 Genes, Genomes, Genetics 8:123–130.

716 Hamilton, W. D. 1967. Extraordinary sex ratios. Science 156:477–488.

717 Hartl, D. L. 1970. Analysis of a general population genetic model of meiotic drive. Evolution
718 24:538–545.

719 ———. 1972. Population dynamics of sperm and pollen killers. Theoretical and Applied Genetics
720 42:81–88.

721 Henikoff, S., K. Ahmad, and H. S. Malik. 2001. The centromere paradox: stable inheritance with
722 rapidly evolving DNA. Science 293:1098–1102.

723 Hiraizumi, Y. 1962. Distorted segregation and genetic load. The Japanese Journal of Genetics
724 37:147–154.

725 Holman, L., T. A. Price, N. Wedell, and H. Kokko. 2015. Coevolutionary dynamics of polyandry
726 and sex-linked meiotic drive. Evolution 69:709–720.

727 Holsinger, K. E., M. W. Feldman, and F. B. Christiansen. 1984. The evolution of self-fertilization
728 in plants: a population genetic model. The American Naturalist 124:446–453.

729 Hu, W., Z.-D. Jiang, F. Suo, J.-X. Zheng, W.-Z. He, and L.-L. Du. 2017. A large gene family in
730 fission yeast encodes spore killers that subvert Mendel's law. Elife 6:e26057.

731 Hurst, G. D. D., and J. H. Werren. 2001. The role of selfish genetic elements in eukaryotic
732 evolution. Nature Reviews Genetics 2:597–606.

733 Kimura, M. 1962. On the probability of fixation of mutant genes in a population. Genetics
734 47:713–719.

735 Kyrou, K., A. M. Hammond, R. Galizi, N. Kranjc, A. Burt, A. K. Beaghton, T. Nolan, and
736 A. Crisanti. 2018. A CRISPR–Cas9 gene drive targeting doublesex causes complete population
737 suppression in caged *Anopheles gambiae* mosquitoes. Nature Biotechnology 36:1062–1066.

738 Larracuente, A. M., and D. C. Presgraves. 2012. The selfish *Segregation Distorter* gene complex
739 of *Drosophila melanogaster*. Genetics 192:33–53.

740 Lewontin, R. C. 1968. The effect of differential viability on the population dynamics of t alleles
741 in the house mouse. Evolution 22:262–273.

742 Lewontin, R. C., and L. C. Dunn. 1960. The evolutionary dynamics of a polymorphism in the
743 house mouse. Genetics 45:705–722.

744 Lindholm, A. K., K. A. Dyer, R. C. Firman, L. Fishman, W. Forstmeier, L. Holman, H. Johan-
745 nesson, U. Knief, H. Kokko, A. M. Larracuente, et al. 2016. The ecology and evolutionary
746 dynamics of meiotic drive. Trends in Ecology & Evolution 31:315–326.

747 Lyttle, T. W. 1991. Segregation distorters. Annual Review of Genetics 25:511–581.

748 ———. 1993. Cheaters sometimes prosper: distortion of mendelian segregation by meiotic drive.
749 Trends in Genetics 9:205–210.

750 Meade, L. C., D. Dinneen, R. Kad, D. M. Lynch, K. Fowler, and A. Pomiankowski. 2019. Ejaculate
751 sperm number compensation in stalk-eyed flies carrying a selfish meiotic drive element. Heredity
752 122:916–926.

753 Nauta, M. J., and R. F. Hoekstra. 1993. Evolutionary dynamics of spore killers. Genetics 135:923–
754 930.

755 Nieuwenhuis, B. P. S., and T. Y. James. 2016. The frequency of sex in fungi. Philosophical
756 Transactions of the Royal Society B: Biological Sciences 371:20150540.

757 Nuckolls, N. L., M. A. B. Núñez, M. T. Eickbush, J. M. Young, J. J. Lange, S. Y. Jonathan,
758 G. R. Smith, S. L. Jaspersen, H. S. Malik, and S. E. Zanders. 2017. *wtf* genes are prolific dual
759 poison-antidote meiotic drivers. Elife 6:e26033.

760 Núñez, M. A. B., I. M. Sabbarini, M. T. Eickbush, Y. Liang, J. J. Lange, A. M. Kent, and S. E.
761 Zanders. 2020. Dramatically diverse *Schizosaccharomyces pombe wtf* meiotic drivers all display
762 high gamete-killing efficiency. PLoS Genetics 16:e1008350.

763 Otto, S. P., and T. Day. 2011. A biologist's guide to mathematical modeling in ecology and
764 evolution. Princeton University Press, Princeton.

765 Padieu, E., and J. Bernet. 1967. Mode d'action des gènes responsables de l'avortement de certains
766 produits de la méiose chez l'Ascomycète *Podospora anserina*. Compte Rendu Hebdomadaire
767 des Séances de l'Académie des Sciences Série D:2300–2303.

768 Pinzone, C. A., and K. A. Dyer. 2013. Association of polyandry and sex-ratio drive prevalence in
769 natural populations of *Drosophila neotestacea*. Proceedings of the Royal Society B: Biological
770 Sciences 280:20131397.

771 Raju, N. B. 1994. Ascomycete spore killers: chromosomal elements that distort genetic ratios
772 among the products of meiosis. Mycologia 86:461–473.

773 Rice, W. R. 2013. Nothing in genetics makes sense except in light of genomic conflict. Annual
774 Review of Ecology, Evolution, and Systematics 44:217–237.

775 Sandler, L., and E. Novitski. 1957. Meiotic drive as an evolutionary force. The American Naturalist
776 91:105–110.

777 Silar, P. 2013. *Podospora anserina*: from laboratory to biotechnology. Pages 283–309 *in* Genomics
778 of Soil-and Plant-Associated Fungi. Springer.

779 Silver, L. M. 1985. Mouse *t* haplotypes. Annual Review of Genetics 19:179–208.

780 Svedberg, J., A. A. Vogan, N. A. Rhoades, D. Sarmarajeewa, D. J. Jacobson, M. Lascoux, T. M.
781 Hammond, and H. Johannesson. 2020. An introgressed gene causes meiotic drive in *Neurospora*
782 *sitophila*. bioRxiv doi:10.1101/2020.01.29.923946.

783 Sweigart, A. L., Y. Brandvain, and L. Fishman. 2019. Making a murderer: the evolutionary
784 framing of hybrid gamete-killers. Trends in Genetics 35:245–252.

785 Turner, B. C., and D. D. Perkins. 1979. Spore killer, a chromosomal factor in *Neurospora* that
786 kills meiotic products not containing it. Genetics 93:587–606.

787 Tusso, S., B. P. Nieuwenhuis, F. J. Sedlazeck, J. W. Davey, D. C. Jeffares, and J. B. Wolf. 2019.
788 Ancestral admixture is the main determinant of global biodiversity in fission yeast. Molecular
789 Biology and Evolution 36:1975–1989.

van der Gaag, M. 2005. Genomic conflicts in *Podospora anserina*= Genomische conflicten in *Podospora anserina*. Thesis Wageningen University.

van der Gaag, M., A. J. M. Debets, J. Oosterhof, M. Slakhorst, J. A. G. M. Thijssen, and R. F. Hoekstra. 2000. Spore-killing meiotic drive factors in a natural population of the fungus *Podospora anserina*. Genetics 156:593–605.

Vogan, A. A., S. L. Ament-Velásquez, E. Bastiaans, O. Wallerman, S. J. Saupe, A. Suh, and H. Johannesson. 2020. *The Enterprise*: A massive transposon carrying *Spok* meiotic drive genes. bioRxiv doi:10.1101/2020.03.25.007153.

Vogan, A. A., S. L. Ament-Velásquez, A. Granger-Farbos, J. Svedberg, E. Bastiaans, A. J. Debets, V. Coustou, H. Yvanne, C. Clavé, S. J. Saupe, et al. 2019. Combinations of *Spok* genes create multiple meiotic drivers in *Podospora*. Elife 8:e46454.

Werren, J. H. 2011. Selfish genetic elements, genetic conflict, and evolutionary innovation. Proceedings of the National Academy of Sciences 108:10863–10870.

Zanders, S. E., M. T. Eickbush, S. Y. Jonathan, J.-W. Kang, K. R. Fowler, G. R. Smith, and H. S. Malik. 2014. Genome rearrangements and pervasive meiotic drive cause hybrid infertility in fission yeast. Elife 3:e02630.

Supplementary Material

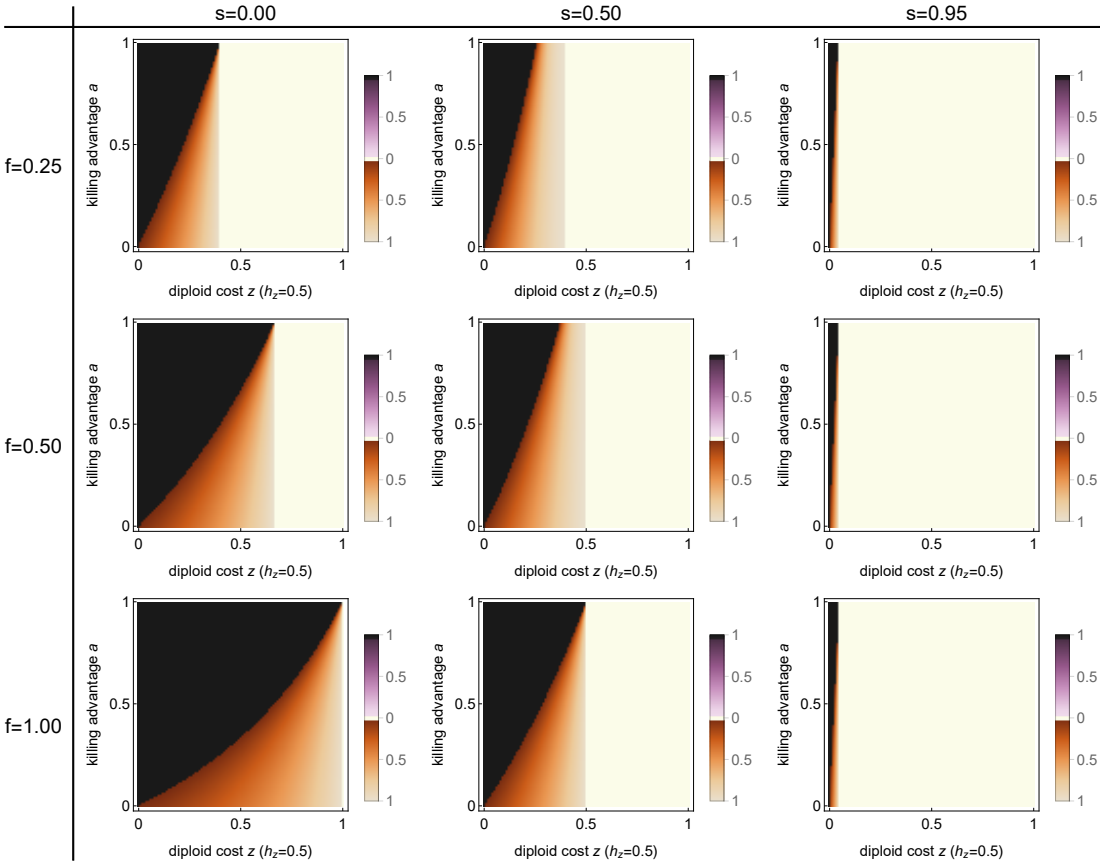

Figure S1: **Bifurcation analysis of the *Podospora* model with additive ($h_z = 0.5$) diploid fitness costs** z. Diploid fitness costs z, killing advantage a, selfing rate s and probability of first-division segregation f are bifurcation parameters. Extinction ($\hat{p}_D = 0$) and fixation ($\hat{p}_D = 1$) of the killer allele D always constitute equilibria. Additionally, one interior equilibrium is possible. Parameter regions are color coded as follows: **white**, D cannot invade and $\hat{p}_D = 0$ is a globally stable equilibrium; **black**, D can invade and reach fixation, $\hat{p}_D = 1$ is a globally stable equilibrium; **purple**, D can invade but cannot reach fixation and coexists with the non-killing allele d at a globally stable interior equilibrium $0 < \hat{p}_D < 1$, whose value is given by the shade of purple; **brown**, the two boundary equilibria $\hat{p}_D = 0$ and $\hat{p}_D = 1$ are stable and separated by an unstable interior equilibrium $0 < \hat{p}_D < 1$, whose value is given by the shade of brown. Each panel is based on 100x100 parameter combinations. Other fixed parameters: $e = 1$, $m = 0$, other fitness costs to zero.

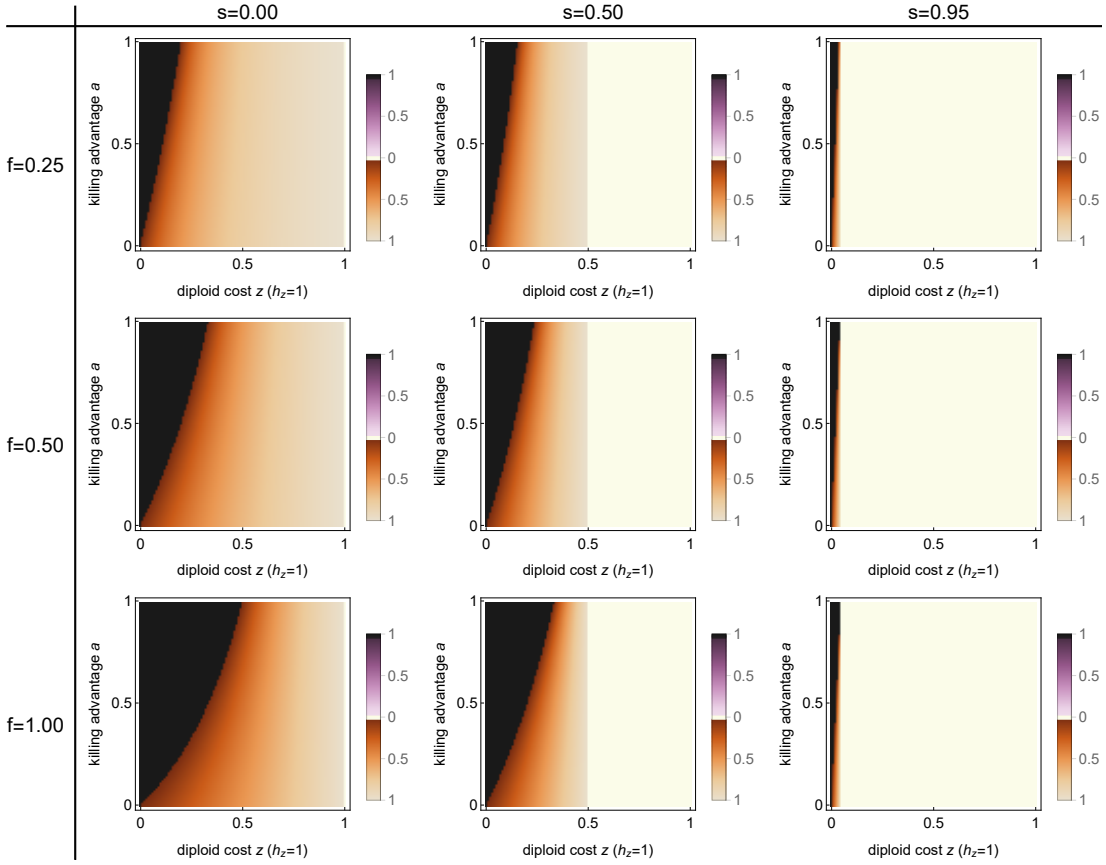

Figure S2: **Bifurcation analysis of the *Podospora* model with dominant ($h_z = 1$) diploid fitness costs** z. Diploid fitness costs z, killing advantage a, selfing rate s and probability of first-division segregation f are bifurcation parameters. Extinction ($\hat{p}_D = 0$) and fixation ($\hat{p}_D = 1$) of the killer allele D always constitute equilibria. Additionally, one interior equilibrium is possible. Parameter regions are color coded as follows: **white**, D cannot invade and $\hat{p}_D = 0$ is a globally stable equilibrium; **black**, D can invade and reaches fixation, $\hat{p}_D = 1$ is a globally stable equilibrium; **purple**, D can invade but cannot reach fixation and coexists with the non-killing allele d at a globally stable interior equilibrium $0 < \hat{p}_D < 1$, whose value is given by the shade of purple; **brown**, the two boundary equilibria $\hat{p}_D = 0$ and $\hat{p}_D = 1$ are stable and separated by an unstable interior equilibrium $0 < \hat{p}_D < 1$, whose value is given by the shade of brown. Each panel is based on 100x100 parameter combinations. Other fixed parameters: $e = 1$, $m = 0$, other fitness costs to zero.

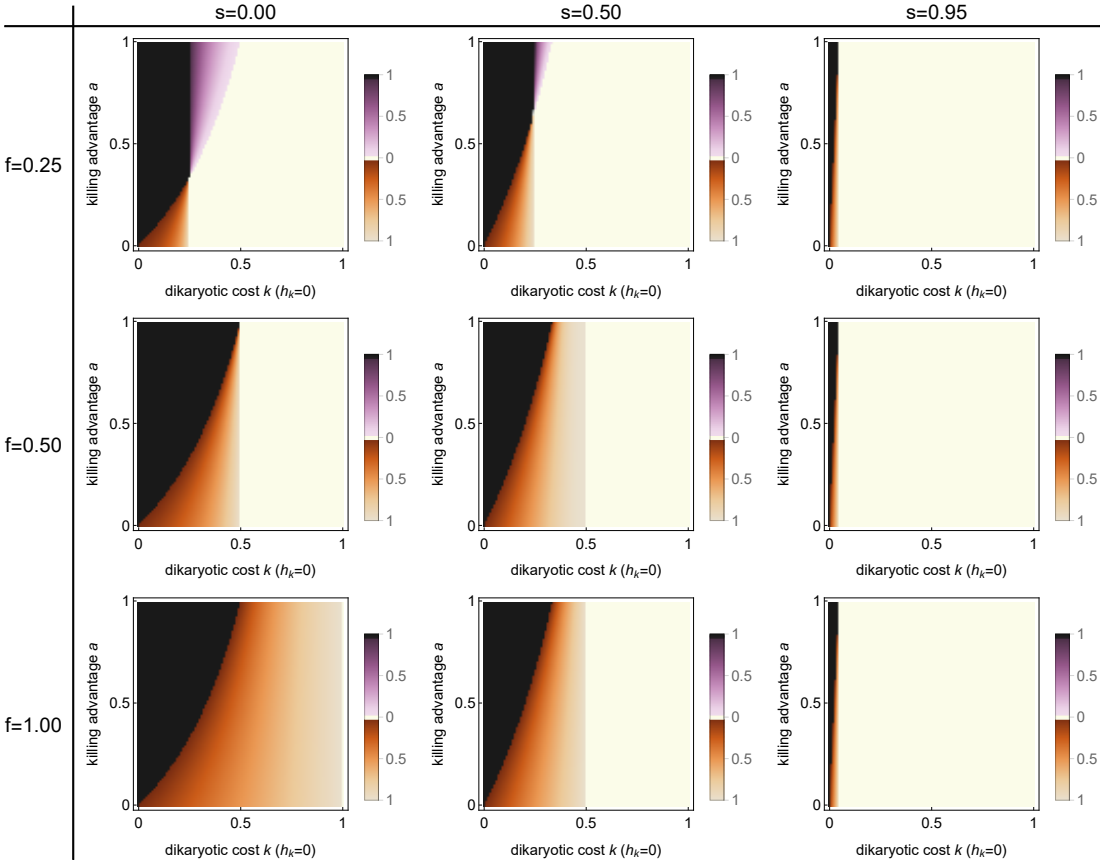

Figure S3: **Bifurcation analysis of the *Podospora* model with recessive ($h_k = 0$) dikaryotic fitness costs** k. Dikaryotic fitness costs k, killing advantage a, selfing rate s and probability of first-division segregation f are bifurcation parameters. Extinction ($\hat{p}_D = 0$) and fixation ($\hat{p}_D = 1$) of the killer allele D always constitute equilibria. Additionally, one interior equilibrium is possible. Parameter regions are color coded as follows: **white**, D cannot invade and $\hat{p}_D = 0$ is a globally stable equilibrium; **black**, D can invade and reaches fixation, $\hat{p}_D = 1$ is a globally stable equilibrium; **purple**, D can invade but cannot reach fixation and coexists with the non-killing allele d at a globally stable interior equilibrium $0 < \hat{p}_D < 1$, whose value is given by the shade of purple; **brown**, the two boundary equilibria $\hat{p}_D = 0$ and $\hat{p}_D = 1$ are stable and separated by an unstable interior equilibrium $0 < \hat{p}_D < 1$, whose value is given by the shade of brown. Each panel is based on 100x100 parameter combinations. Other fixed parameters: $e = 1$, $m = 0$, other fitness costs to zero.

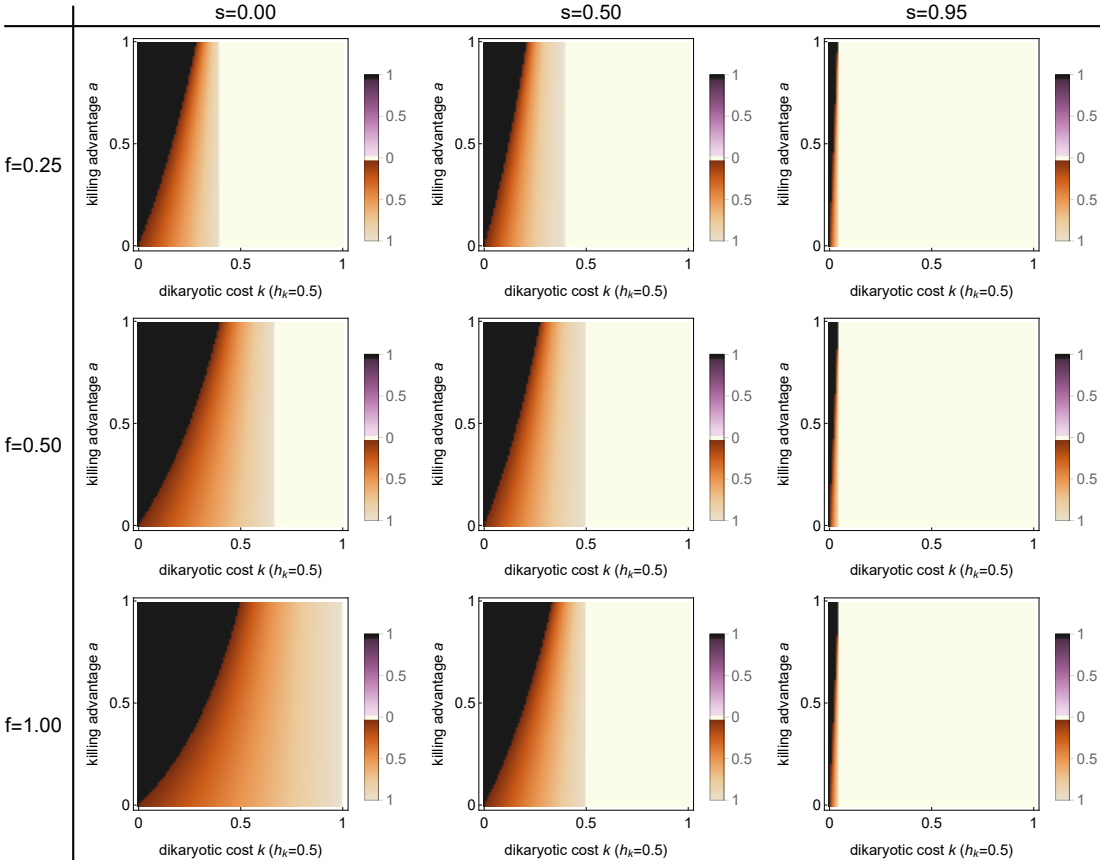

Figure S4: **Bifurcation analysis of the *Podospora* model with additive ($h_k = 0.5$) dikaryotic fitness costs** k. Dikaryotic fitness costs k, killing advantage a, selfing rate s and probability of first-division segregation f are bifurcation parameters. Extinction ($\hat{p}_D = 0$) and fixation ($\hat{p}_D = 1$) of the killer allele D always constitute equilibria. Additionally, one interior equilibrium is possible. Parameter regions are color coded as follows: **white**, D cannot invade and $\hat{p}_D = 0$ is a globally stable equilibrium; **black**, D can invade and reaches fixation, $\hat{p}_D = 1$ is a globally stable equilibrium; **purple**, D can invade but cannot reach fixation and coexists with the non-killing allele d at a globally stable interior equilibrium $0 < \hat{p}_D < 1$, whose value is given by the shade of purple; **brown**, the two boundary equilibria $\hat{p}_D = 0$ and $\hat{p}_D = 1$ are stable and separated by an unstable interior equilibrium $0 < \hat{p}_D < 1$, whose value is given by the shade of brown. Each panel is based on 100x100 parameter combinations. Other fixed parameters: $e = 1$, $m = 0$, other fitness costs to zero.

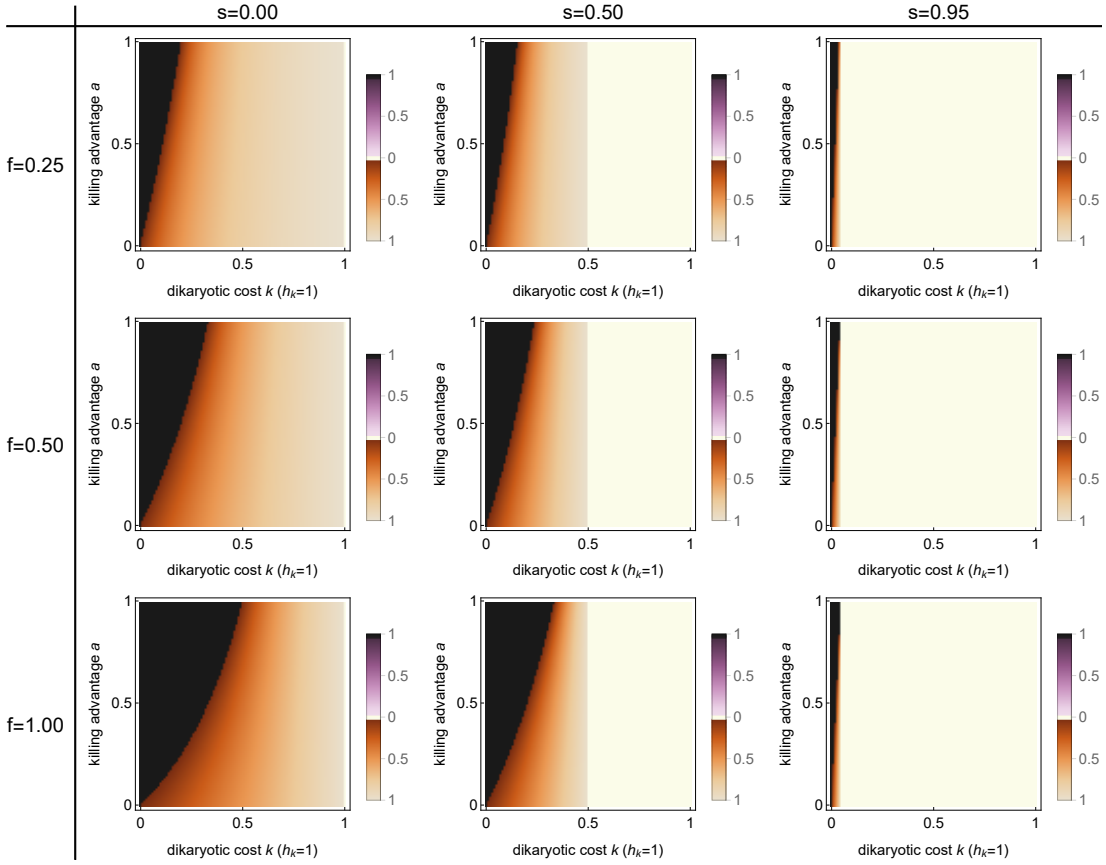

Figure S5: **Bifurcation analysis of the *Podospora* model with dominant ($h_k = 1$) dikaryotic fitness costs** k. Dikaryotic fitness costs k, killing advantage a, selfing rate s and probability of first-division segregation f are bifurcation parameters. Extinction ($\hat{p}_D = 0$) and fixation ($\hat{p}_D = 1$) of the killer allele D always constitute equilibria. Additionally, one interior equilibrium is possible. Parameter regions are color coded as follows: **white**, D cannot invade and $\hat{p}_D = 0$ is a globally stable equilibrium; **black**, D can invade and reaches fixation, $\hat{p}_D = 1$ is a globally stable equilibrium; **purple**, D can invade but cannot reach fixation and coexists with the non-killing allele d at a globally stable interior equilibrium $0 < \hat{p}_D < 1$, whose value is given by the shade of purple; **brown**, the two boundary equilibria $\hat{p}_D = 0$ and $\hat{p}_D = 1$ are stable and separated by an unstable interior equilibrium $0 < \hat{p}_D < 1$, whose value is given by the shade of brown. Each panel is based on 100x100 parameter combinations. Other fixed parameters: $e = 1$, $m = 0$, other fitness costs to zero.

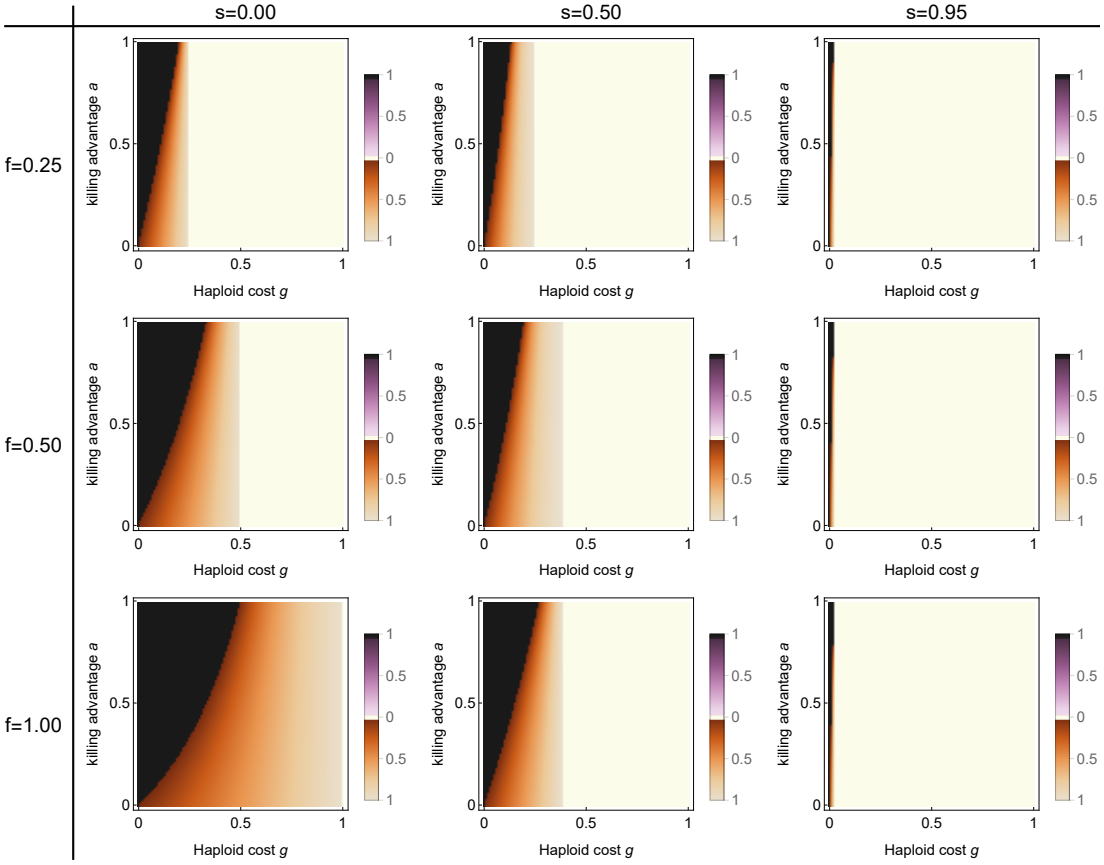

Figure S6: **Bifurcation analysis of the *Podospora* model with haploid fitness costs** g. Haploid fitness costs g, killing advantage a, selfing rate s and probability of first-division segregation f are bifurcation parameters. Extinction ($\hat{p}_D = 0$) and fixation ($\hat{p}_D = 1$) of the killer allele D always constitute equilibria. Additionally, one interior equilibrium is possible. Parameter regions are color coded as follows: **white**, D cannot invade and $\hat{p}_D = 0$ is a globally stable equilibrium; **black**, D can invade and reaches fixation, $\hat{p}_D = 1$ is a globally stable equilibrium; **purple**, D can invade but cannot reach fixation and coexists with the non-killing allele d at a globally stable interior equilibrium $0 < \hat{p}_D < 1$, whose value is given by the shade of purple; **brown**, the two boundary equilibria $\hat{p}_D = 0$ and $\hat{p}_D = 1$ are stable and separated by an unstable interior equilibrium $0 < \hat{p}_D < 1$, whose value is given by the shade of brown. Each panel is based on 100x100 parameter combinations. Other fixed parameters: $e = 1$, $m = 0$, other fitness costs to zero.

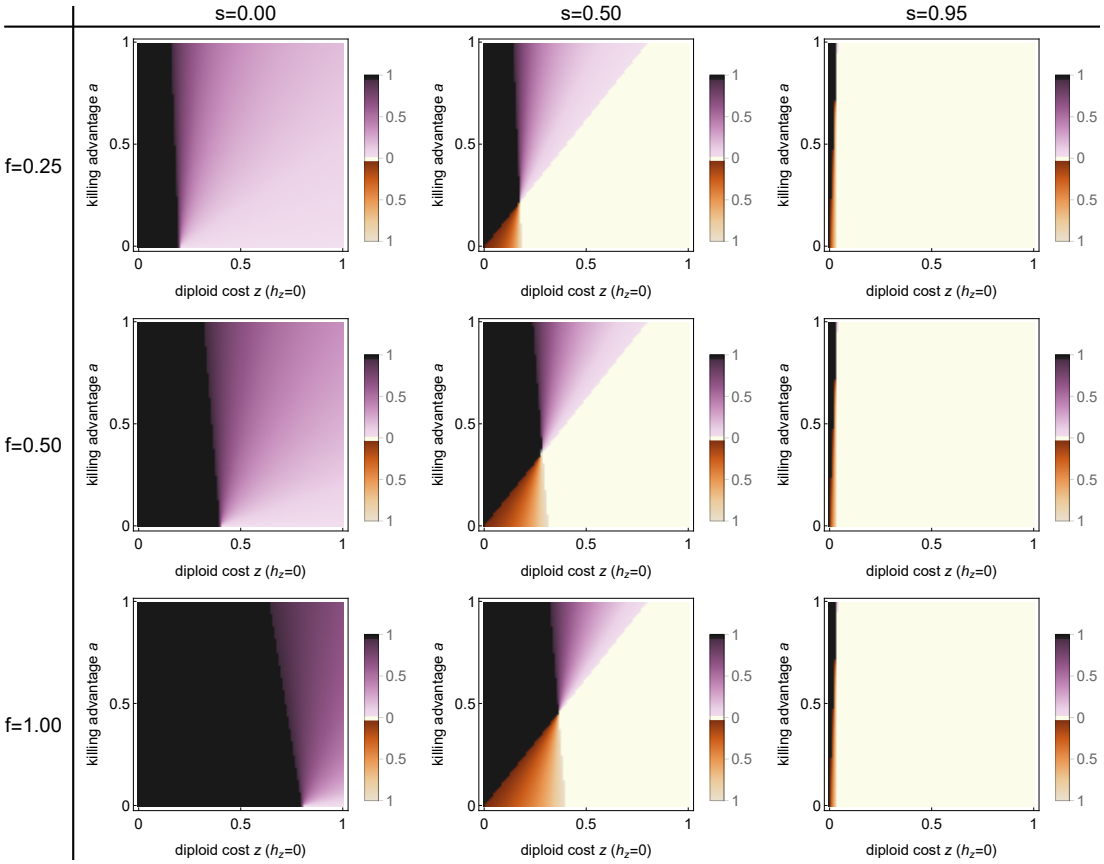

Figure S7: **Bifurcation analysis of the *Podospora* model with incomplete killing efficiency ($e = 80\%$) and recessive ($h_z = 0$) diploid fitness costs** z. Diploid fitness costs z, killing advantage a, selfing rate s and probability of first-division segregation f are bifurcation parameters. Extinction ($\hat{p}_D = 0$) and fixation ($\hat{p}_D = 1$) of the killer allele D always constitute equilibria. Additionally, one interior equilibrium is possible. Parameter regions are color coded as follows: **white**, D cannot invade and $\hat{p}_D = 0$ is a globally stable equilibrium; **black**, D can invade and reaches fixation, $\hat{p}_D = 1$ is a globally stable equilibrium; **purple**, D can invade but cannot reach fixation and coexists with the non-killing allele d at a globally stable interior equilibrium $0 < \hat{p}_D < 1$, whose value is given by the shade of purple; **brown**, the two boundary equilibria $\hat{p}_D = 0$ and $\hat{p}_D = 1$ are stable and separated by an unstable interior equilibrium $0 < \hat{p}_D < 1$, whose value is given by the shade of brown. Each panel is based on 100x100 parameter combinations. Fixed parameters: $m = 0$, other fitness costs to zero.

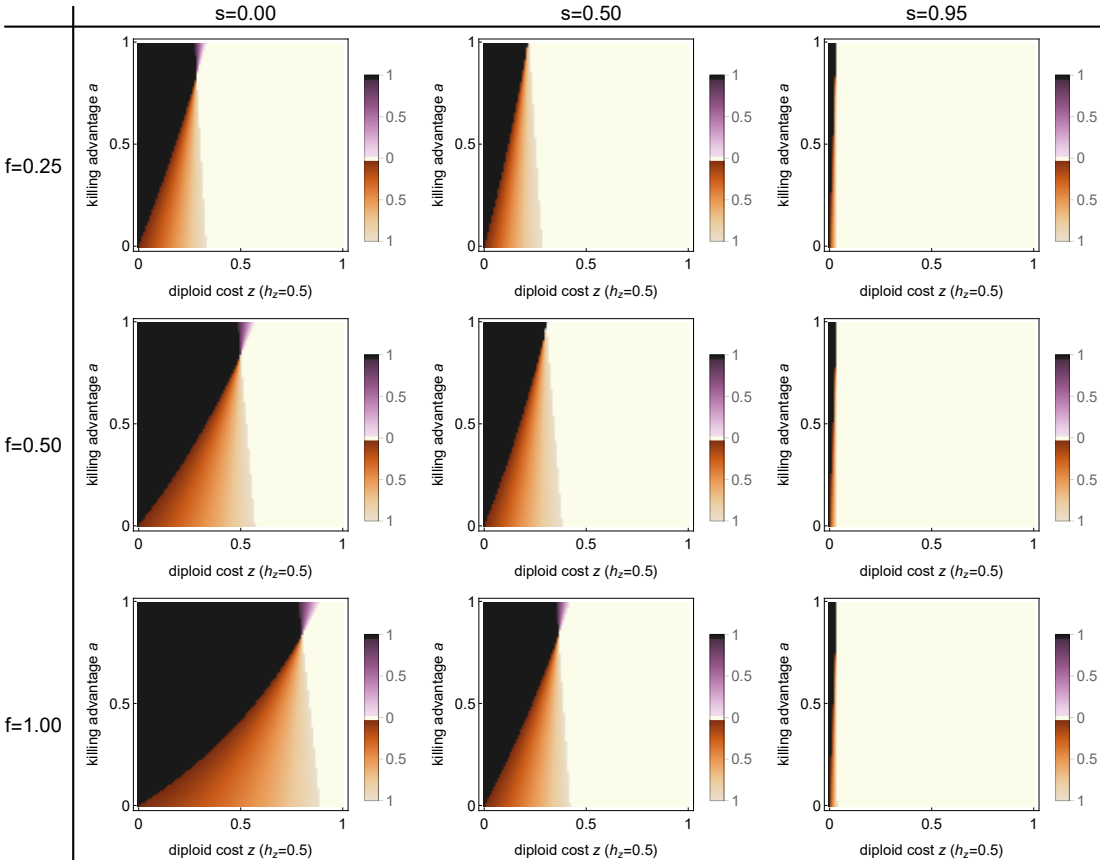

Figure S8: **Bifurcation analysis of the *Podospora* model with incomplete killing efficiency** ($e = 80\%$) **and additive** ($h_z = 0.5$) **diploid fitness costs** z. Diploid fitness costs z, killing advantage a, selfing rate s and probability of first-division segregation f are bifurcation parameters. Extinction ($\hat{p}_D = 0$) and fixation ($\hat{p}_D = 1$) of the killer allele D always constitute equilibria. Additionally, one interior equilibrium is possible. Parameter regions are color coded as follows: **white**, D cannot invade and $\hat{p}_D = 0$ is a globally stable equilibrium; **black**, D can invade and reaches fixation, $\hat{p}_D = 1$ is a globally stable equilibrium; **purple**, D can invade but cannot reach fixation and coexists with the non-killing allele d at a globally stable interior equilibrium $0 < \hat{p}_D < 1$, whose value is given by the shade of purple; **brown**, the two boundary equilibria $\hat{p}_D = 0$ and $\hat{p}_D = 1$ are stable and separated by an unstable interior equilibrium $0 < \hat{p}_D < 1$, whose value is given by the shade of brown. Each panel is based on 100x100 parameter combinations. Fixed parameters: $m = 0$, other fitness costs to zero.

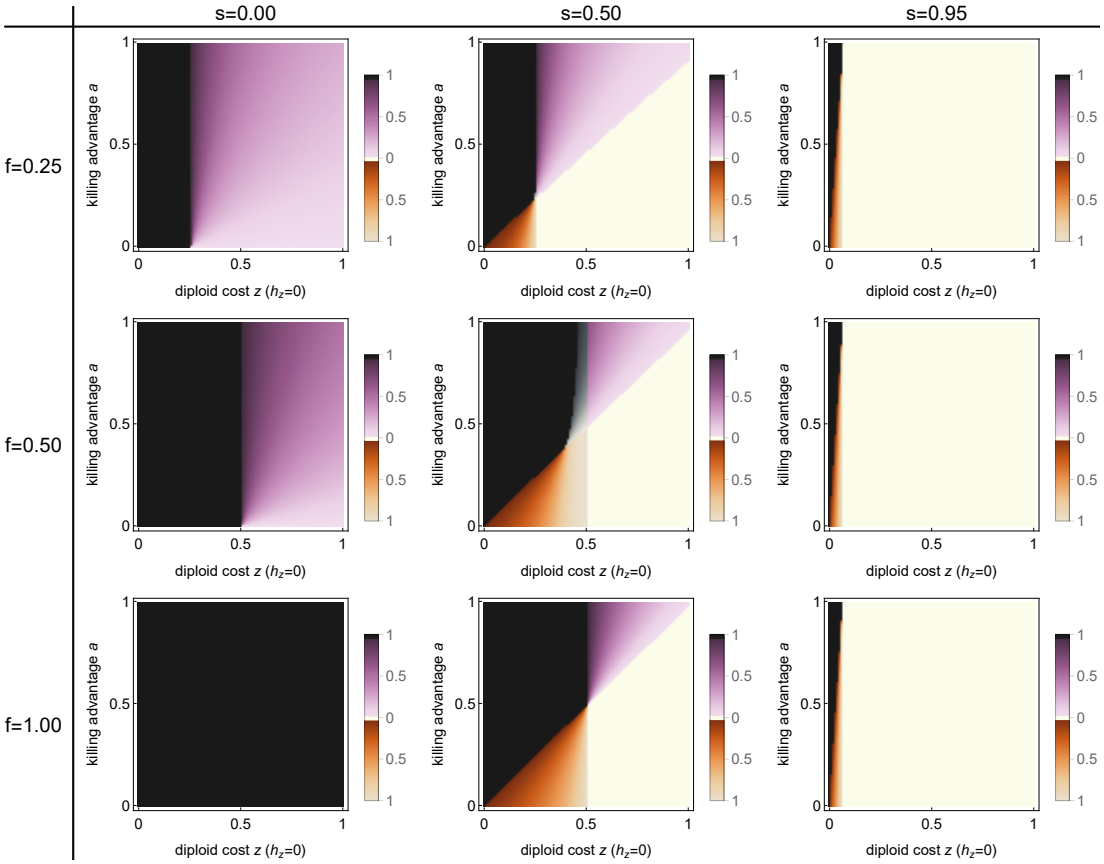

Figure S9: **Bifurcation analysis of the *Podospora* model with monokaryons in 5% of asci ($m = 0.05$) and recessive ($h_z = 0$) diploid fitness costs** z. Diploid fitness costs z, killing advantage a, selfing rate s and probability of first-division segregation f are bifurcation parameters. Extinction ($\hat{p}_D = 0$) and fixation ($\hat{p}_D = 1$) of the killer allele D always constitute equilibria. Additionally, one interior equilibria is possible. Parameter regions are color coded as follows: **white**, D cannot invade and $\hat{p}_D = 0$ is a globally stable equilibrium; **black**, D can invade and reaches fixation, $\hat{p}_D = 1$ is a globally stable equilibrium; **purple**, D can invade but cannot reach fixation and coexists with the non-killing allele d at a globally stable interior equilibrium $0 < \hat{p}_D < 1$, whose value is given by the shade of purple; **brown**, the two boundary equilibria $\hat{p}_D = 0$ and $\hat{p}_D = 1$ are stable and separated by an unstable interior equilibrium $0 < \hat{p}_D < 1$, whose value is given by the shade of brown. Each panel is based on 100x100 parameter combinations. Fixed parameters: $e = 1$, other fitness costs to zero.

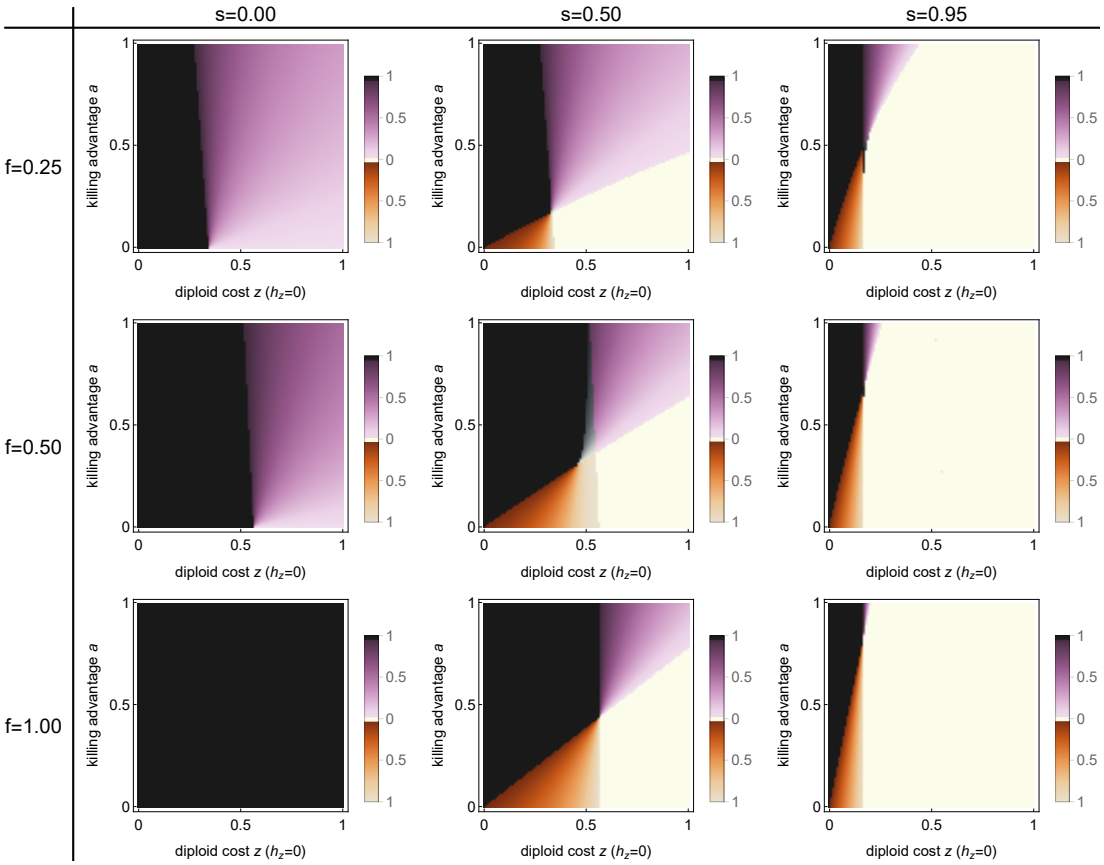

Figure S10: **Bifurcation analysis of the *Podospora* model with monokaryons in 50% of asci ($m = 0.5$) and recessive ($h_z = 0$) diploid fitness costs** z. Diploid fitness costs z, killing advantage a, selfing rate s and probability of first-division segregation f are bifurcation parameters. Extinction ($\hat{p}_D = 0$) and fixation ($\hat{p}_D = 1$) of the killer allele D always constitute equilibria. Additionally, one interior equilibrium is possible. Parameter regions are color coded as follows: **white**, D cannot invade and $\hat{p}_D = 0$ is a globally stable equilibrium; **black**, D can invade and reaches fixation, $\hat{p}_D = 1$ is a globally stable equilibrium; **purple**, D can invade but cannot reach fixation and coexists with the non-killing allele d at a globally stable interior equilibrium $0 < \hat{p}_D < 1$, whose value is given by the shade of purple; **brown**, the two boundary equilibria $\hat{p}_D = 0$ and $\hat{p}_D = 1$ are stable and separated by an unstable interior equilibrium $0 < \hat{p}_D < 1$, whose value is given by the shade of brown; **gray**, two interior equilibria exist, the equilibrium with the lower value is stable, meaning that D can invade and coexist with d at a stable interior equilibrium, whose value is given by the shade of gray. Each panel is based on 100x100 parameter combinations. Fixed parameters: $e = 1$, other fitness costs to zero.

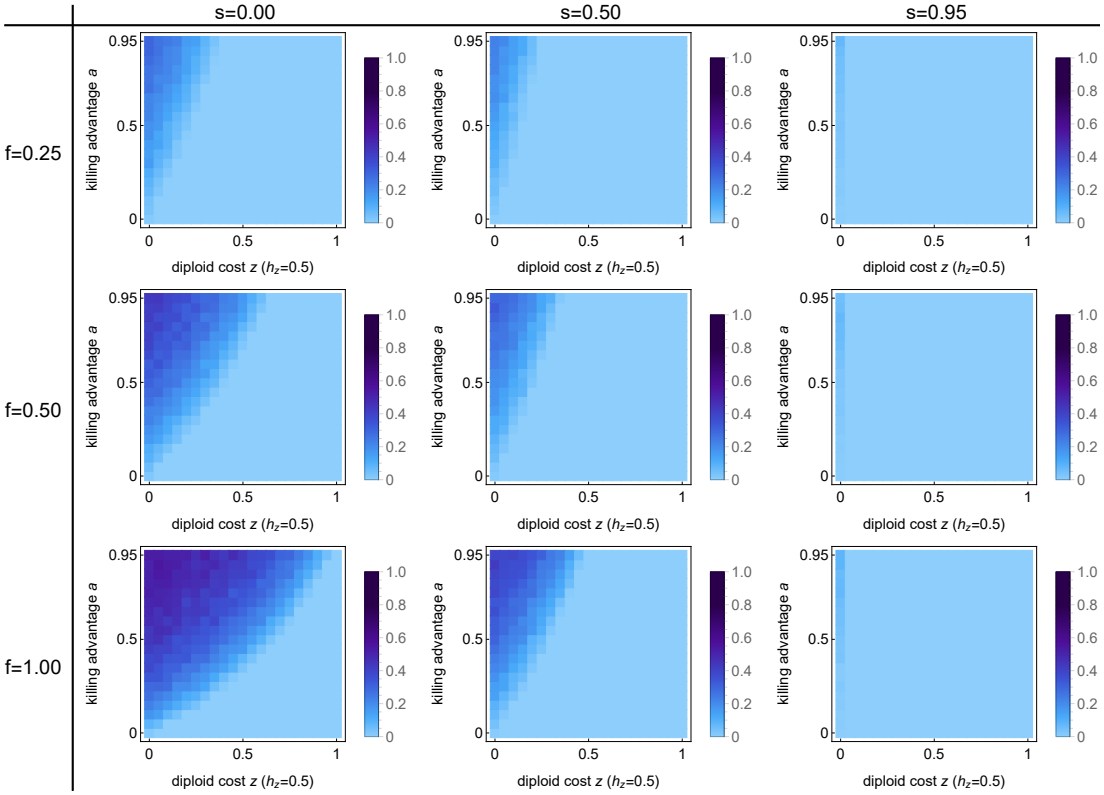

Figure S11: **Invasion probability of a spore killing allele D for the *Podospora* model with additive ($h_z = 0.5$) diploid fitness costs z.** Parameters are the fitness costs z, the killing advantage a, the selfing rate s and the rate of first-division segregation f. Each panel consists of 21x21 parameter combinations and shades of blue indicates the invasion probability estimated from 10^3 stochastic Wright-Fisher simulation runs with a population size of 1000. Other parameters as in Figure S1.

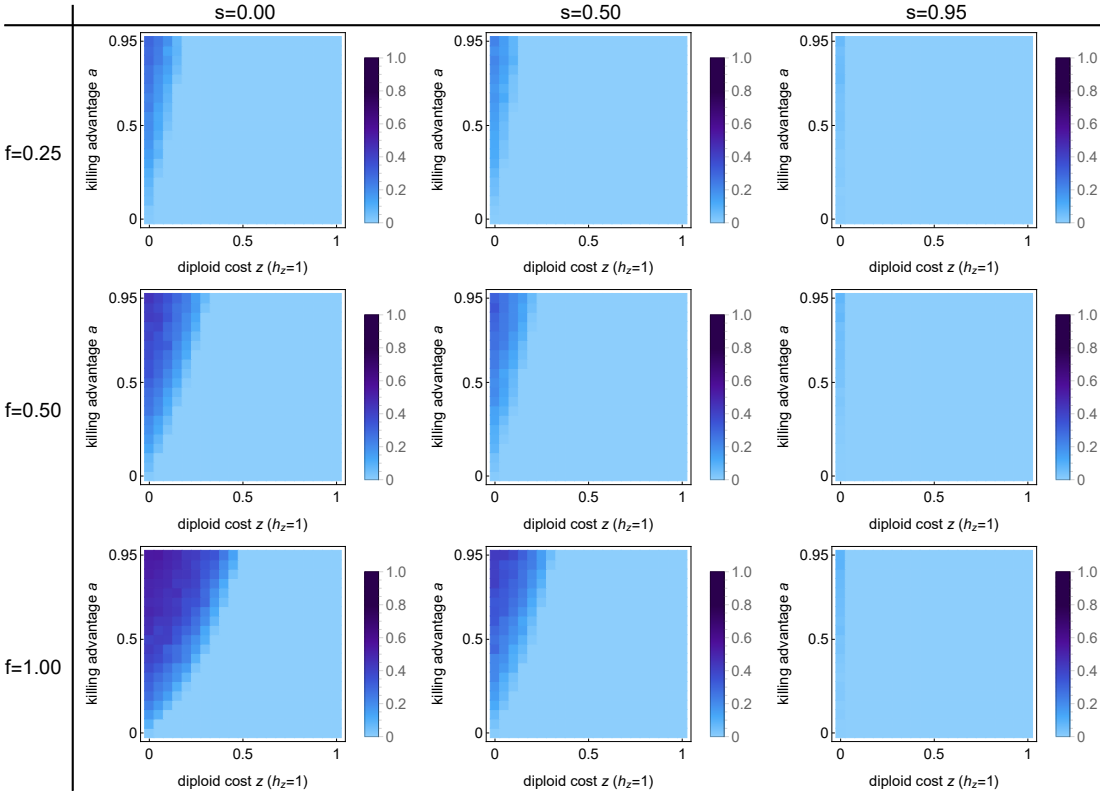

Figure S12: **Invasion probability of a spore killing allele D for the *Podospora* model with dominant ($h_z = 1$) diploid fitness costs z.** Parameters are the fitness costs z, the killing advantage a, the selfing rate s and the rate of first-division segregation f. Each panel consists of 21x21 parameter combinations and shades of blue indicate the invasion probability estimated from 10^3 stochastic Wright-Fisher simulation runs with a population size of 1000. Other parameters as in Figure S2.

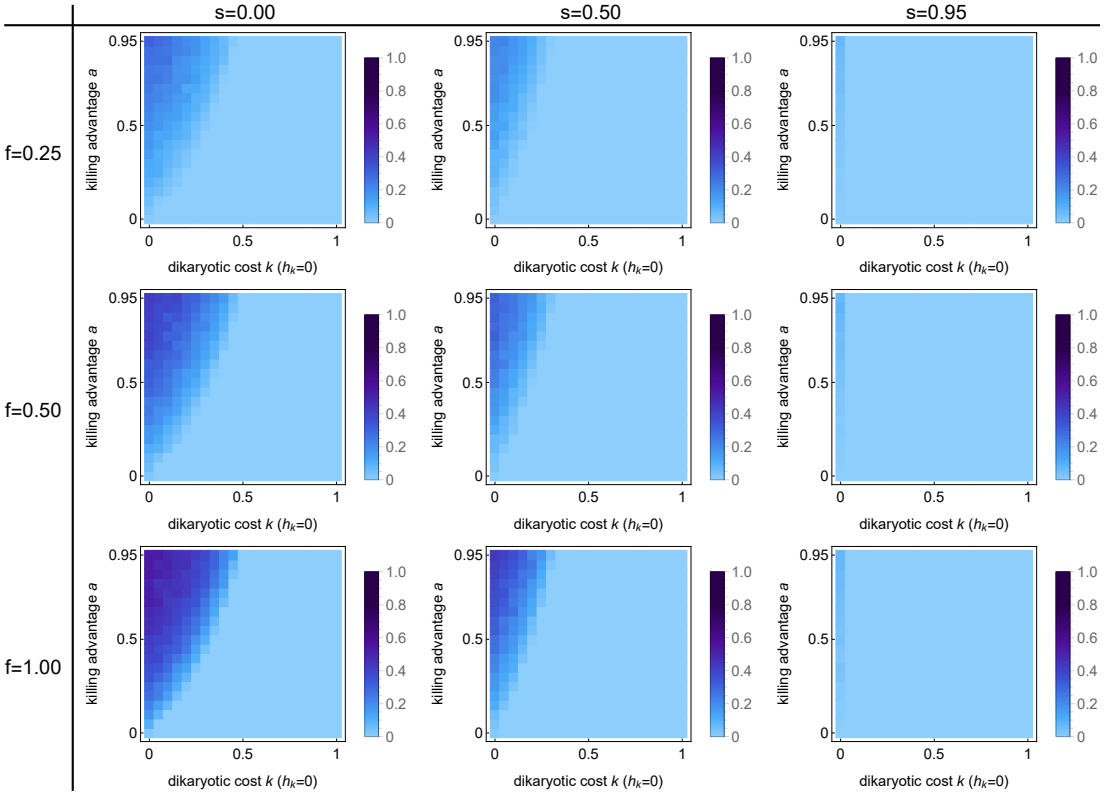

Figure S13: **Invasion probability of a spore killing allele D for the *Podospora* model with recessive ($h_k = 0$) dikaryotic fitness costs k.** Parameters are the fitness costs k, the killing advantage a, the selfing rate s and the rate of first-division segregation f. Each panel consists of 21x21 parameter combinations and shades of blue indicate the invasion probability estimated from 10^3 stochastic Wright-Fisher simulation runs with a population size of 1000. Other parameters as in Figure S3.

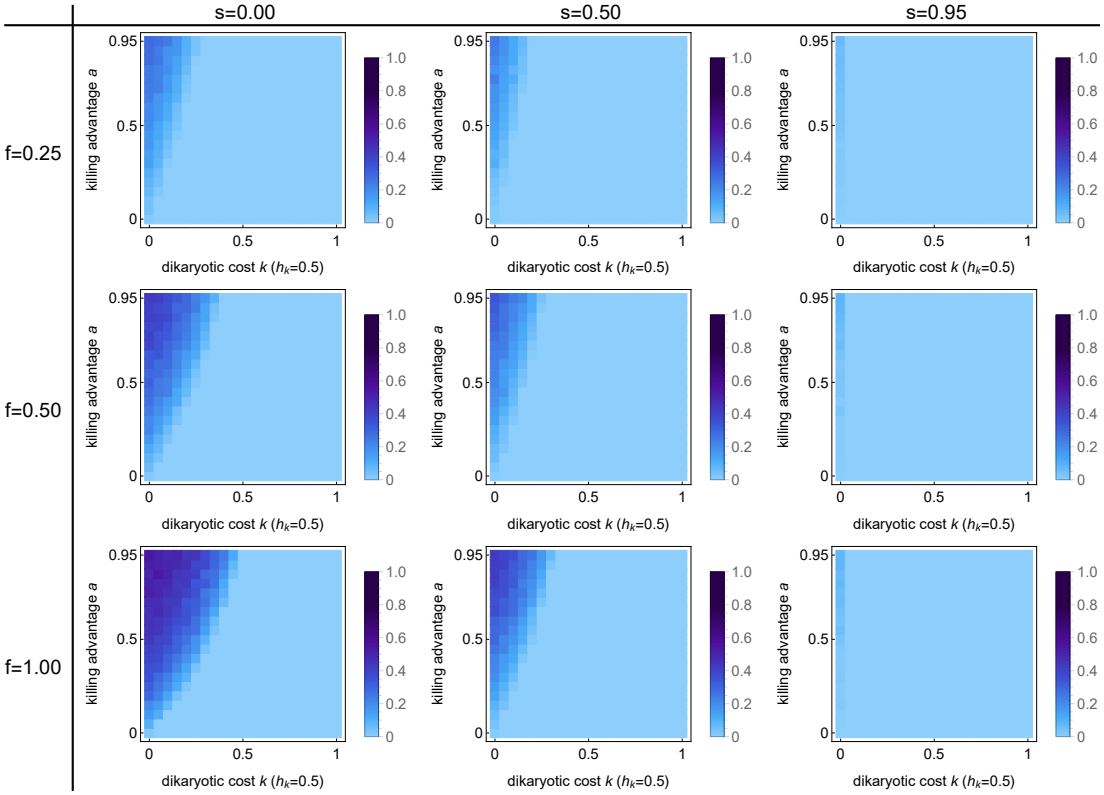

Figure S14: **Invasion probability of a spore killing allele D for the *Podospora* model with additive ($h_k = 1/2$) dikaryotic fitness costs k.** Parameters are the fitness costs k, the killing advantage a, the selfing rate s and the rate of first-division segregation f. Each panel consists of 21x21 parameter combinations and shades of blue indicate the invasion probability estimated from 10^3 stochastic Wright-Fisher simulation runs with a population size of 1000. Other parameters as in Figure S4.

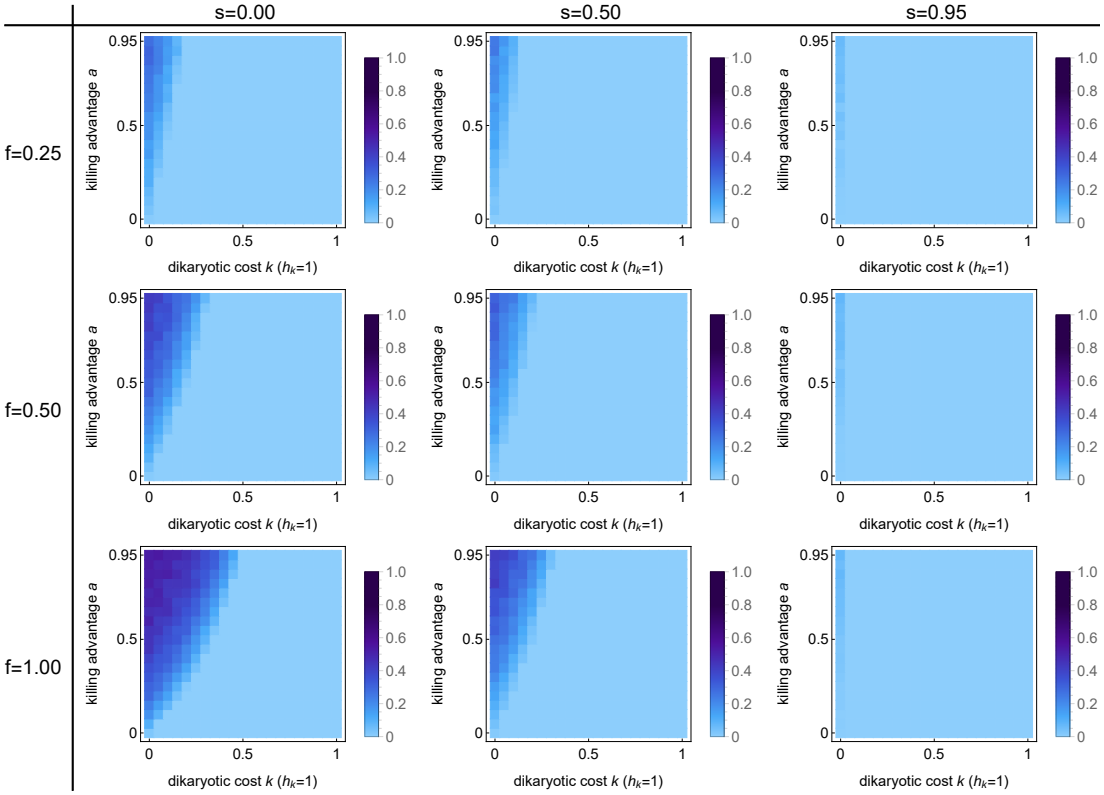

Figure S15: **Invasion probability of a spore killing allele D for the *Podospora* model with dominant ($h_k = 1$) dikaryotic fitness costs k.** Parameters are the fitness costs k, the killing advantage a, the selfing rate s and the rate of first-division segregation f. Each panel consists of 21x21 parameter combinations and shades of blue indicate the invasion probability estimated from 10^3 stochastic Wright-Fisher simulation runs with a population size of 1000. Other parameters as in Figure S5.

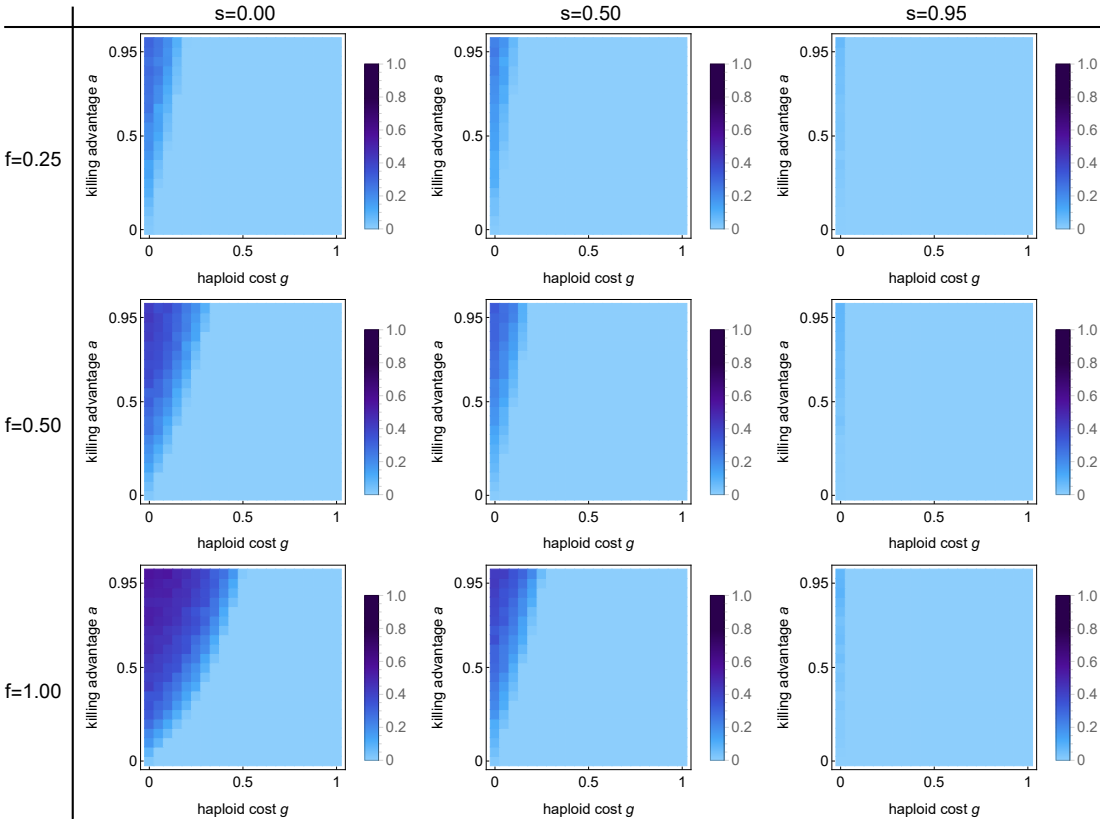

Figure S16: **Invasion probability of a spore killing allele D for the *Podospora* model with haploid fitness costs g.** Parameters are the fitness costs g, the killing advantage a, the selfing rate s and the rate of first-division segregation f. Each panel consists of 21x21 parameter combinations and shades of blue indicate the invasion probability estimated from 10^3 stochastic Wright-Fisher simulation runs with a population size of 1000. Other parameters as in Figure S6.

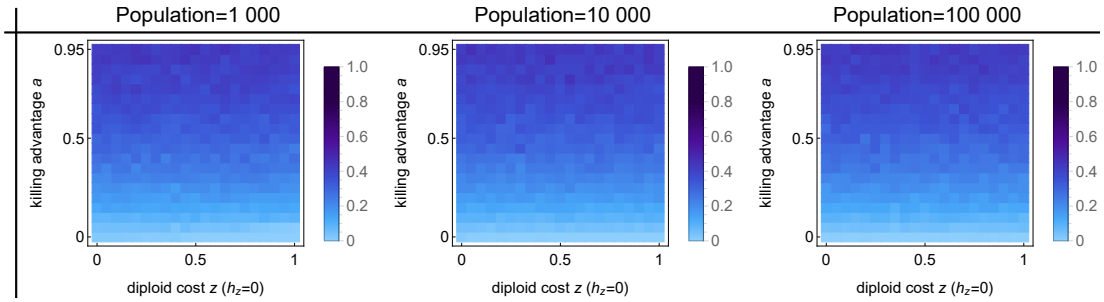

Figure S17: **Effect of population size on invasion probability of a spore killing allele D for the *Podospora* model with recessive diploid costs z.** Parameters are the recessive ($h_z = 0$) fitness costs z, the killing advantage a, and population size.The selfing rate s is fixed to zero and the rate of first-division segregation f to 0.50. Each panel consists of 21x21 parameter combinations and shades of blue indicate the invasion probability estimated from 10^3 stochastic Wright-Fisher simulation runs.

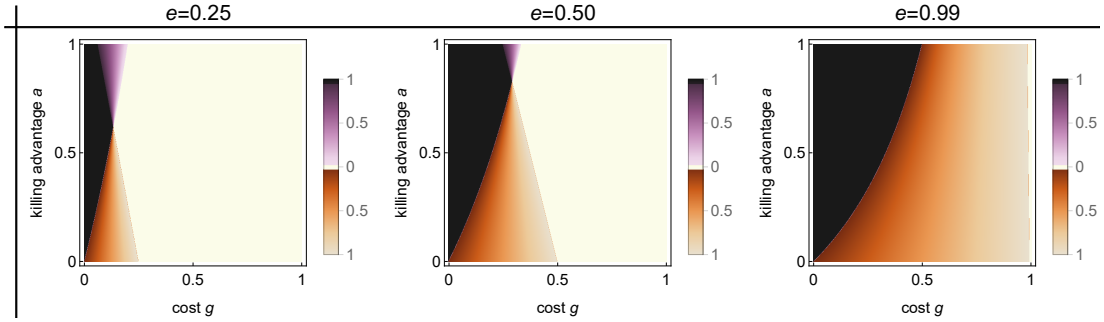

Figure S18: **Bifurcation analysis of the *Neurospora* model with haploid fitness costs** g. Haploid fitness costs g, killing advantage a, and killing efficiency e are bifurcation parameters. Extinction ($\hat{p}_D = 0$) and fixation ($\hat{p}_D = 1$) of the killer allele D always constitute equilibria. Additionally, one interior equilibrium is possible. Parameter regions are color coded as follows: **white**, D cannot invade and $\hat{p}_D = 0$ is a globally stable equilibrium; **black**, D can invade and reaches fixation, $\hat{p}_D = 1$ is a globally stable equilibrium; **purple**, D can invade but cannot reach fixation and coexists with the non-killing allele d at a globally stable interior equilibrium $0 < \hat{p}_D < 1$, whose value is given by the shade of purple; **brown**, the two boundary equilibria $\hat{p}_D = 0$ and $\hat{p}_D = 1$ are stable and separated by an unstable interior equilibrium $0 < \hat{p}_D < 1$, whose value is given by the shade of brown. Each panel is based on 1000x1000 parameter combinations. Fitness costs $z = 0$.

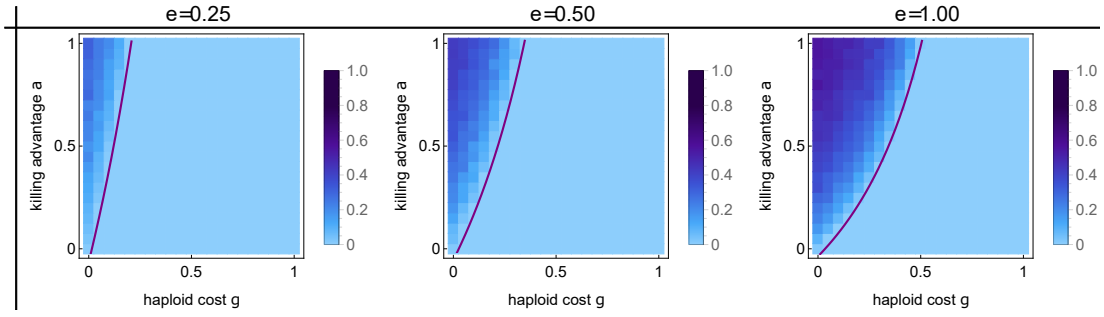

Figure S19: **Invasion probability of a spore killer for the *Neurospora* model with haploid fitness costs** g**.** Parameters are the fitness costs g, the killing advantage a, and the killing efficiency e. Each panel consists of 21x21 parameter combinations and shades of blue indicate the invasion probability estimated from 10^3 stochastic Wright-Fisher simulation runs with a population size of 1000. Parameter combinations to the left and above the purple line allows for invasion of the spore killer according to the deterministic model. Other parameters as in Figure S18.

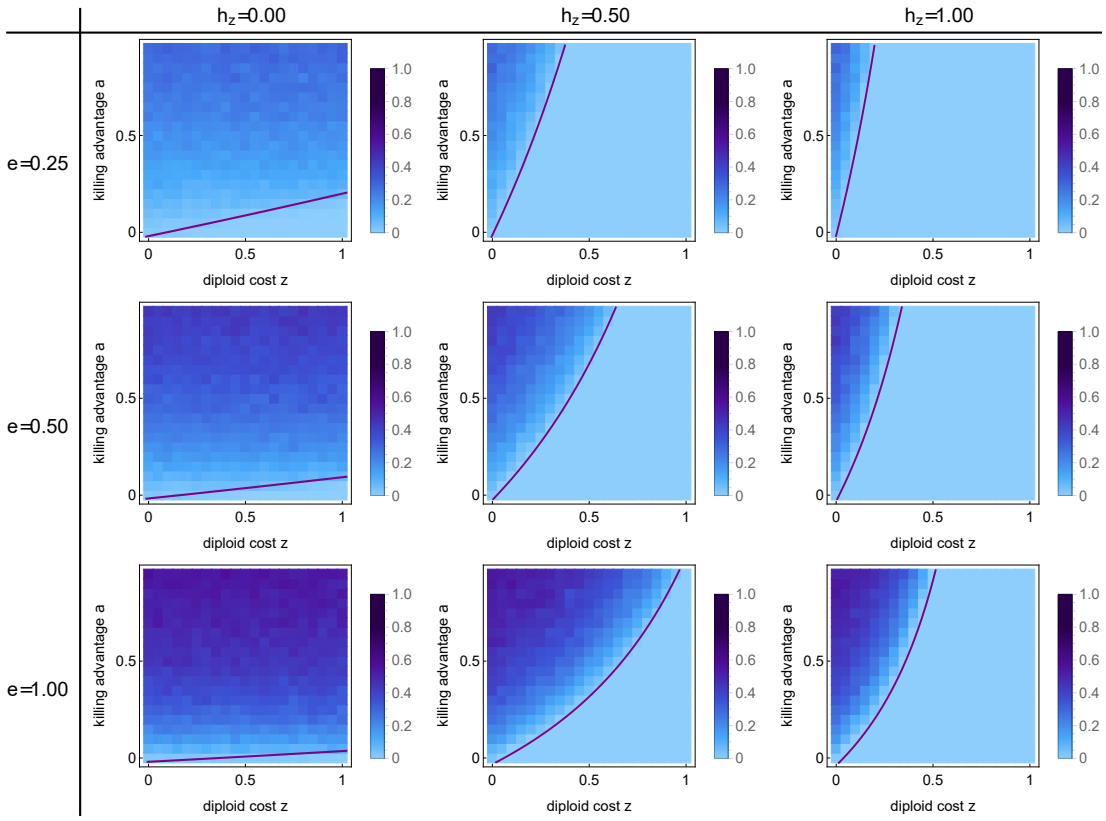

Figure S20: **Invasion probability of a spore killer for the *Neurospora* model with diploid fitness costs z.** Parameters are the fitness costs z, the killing advantage a, the killing efficiency e, and the dominance parameter h_z. Each panel consists of 21x21 parameter combinations and shades of blue indicate the invasion probability estimated from 10^3 stochastic Wright-Fisher simulation runs with a population size of 1000. Parameter combinations to the left and above the purple line allows for invasion of the spore killer according to the deterministic model. Other parameters as in Figure 4.

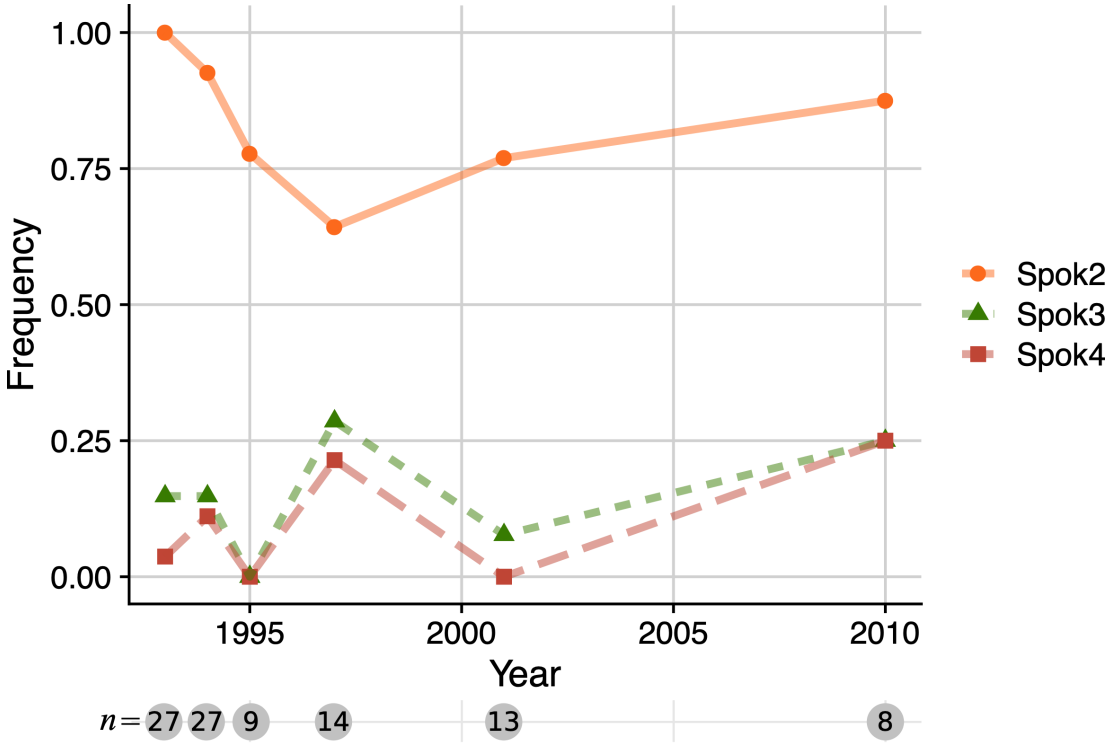

Figure S21: **Frequency of *Spok2*, *Spok3* and *Spok4* in the Wageningen population of *Podospora anserina***. Individuals of *P. anserina* have been collected around Wageningen, The Netherlands, at irregular intervals between 1993 and 2010 (van der Gaag, 2005). The genome of each individual might contain any number and combination of *Spok* genes, from no *Spok* gene to all three of them. The *Spok3* and *Spok4* genes are embedded within a larger haplotype called the '*Spok* block'. Thus, while *Spok3* and *Spok4* can occur on their own, their occurrence seems to be tightly linked. We used published and unpublished genomic data to determine the *Spok* gene content of each individual, and verified that spore killing phenotypes followed expected patterns (Vogan et al., 2019). The number n gives the sample size in each year.

Appendix 1: Comparing absolute and relative meiotic drive

Purpose

In this appendix, we give the details for the model presented in Box 1. To illustrate the qualitative differences in selective advantage between absolute and relative meiotic drive, we built a simple population genetics model somewhat similar to the one presented by Crow (1991). The mechanism of killing advantage or compensation in this model differs slightly from the model presented in the main part to also cover male and female drive systems. The present model allows to vary the efficiency of the drive, which is the proportion of sensitive alleles that are killed during meiosis, and the degree of compensation, which is the proportion of meiotic products suppressed by the action of the meiotic driver (MD) that gets replaced by meiotic products carrying the MD. For example, in a female drive system all suppressed meiotic products are replaced by products carrying the MD (full compensation). In a male drive system, it is possible that some or all of the suppressed sperm cells are replaced (partial compensation). Finally, in a spore killing system, it has been proposed that suppressed meiotic products may be replaced through a mechanism we call killing advantage and which is effectively equivalent to compensation. This simple model aims to clarify the influence of the level of compensation on the dynamics of MDs, with a particular focus on the selective advantage at low frequencies and the invasion probability. Since we are only interested in the effect of different levels of compensation, we focus on the case with no additional fitness costs for the killing allele D. Only suppression of meiotic products from heterozygotes with killing efficiency e and compensation influence the dynamics of the different alleles.

The model

We consider a one-locus drive system with two alleles, the driving allele D and the sensitive allele d. We consider an organism reproducing through random mating. The frequency of the driving and sensitive alleles are p_D and $1-p_D$, respectively. The action of meiotic drive is partitioned into two steps. First, the MD is able to suppress a proportion e ($0 \leq e \leq 1$) of the meiotic products. Then, a fraction c ($0 \leq c \leq e$) of the suppressed meiotic products can be replaced (compensation) by D-carrying products. The model can be summarized by the change of allele frequencies during meiosis as described in Table A1.

Using the information from Table A1, the change in frequency of the driving allele D over one generation is given by

$$p'_D = \frac{p_D^2 + p_D(1-p_D)(1+c)}{1-(e-c)p_D(1-p_D)}, \tag{A1}$$

Table A1: **Genotype frequencies before and after meiosis.** The frequency of the D allele before meiosis is given by p_D, the efficiency of the drive at removing the alternative allele by e, and the propensity of the driving allele to replace suppressed meiotic products by c. Mean fitness $\bar{w}$ is calculated as the sum of the numerators of the entries in the last column of the table.

Genotype (2N)	Frequency		Genotype (N)	Frequency
DD	p_D^2	$\longmapsto$	D	$p_D^2/\bar{w}$
Dd	$2p_D(1-p_D)$	$\nearrow$	D	$p_D(1-p_D)\times(1+c)/\bar{w}$
		$\searrow$	d	$p_D(1-p_D)\times(1-e)/\bar{w}$
dd	$(1-p_D)^2$	$\longmapsto$	d	$(1-p_D)^2/\bar{w}$

where p'_D is the frequency of D at the next generation. We can define the selective advantage s of the driving allele D as

$$1+s=\frac{p'_D}{p_D} \tag{A2}$$

so that a positive s implies that D will increase in frequency. For our model, the selective advantage s of the driving allele equals

$$s=\frac{1+c(1-p_D)}{1-(e-c)p_D(1-p_D)}-1. \tag{A3}$$

The following observations can be made. First, for $p_D<1$ we find that $s>0$. Thus, in a deterministic model the killing allele always increases in frequency. This result holds in particular for the case of no compensation ($c=0$). Second, for $p_D=0$ we find that $s=c$. Thus, for the case of female drive (equivalent to full compensation, $c=1$) we find a maximal value of $s=1$, while for male drive with no compensation $s=0$. A more detailed analysis of the effect of the drive efficiency e and the degree of compensation c is presented in Box 1 in the main manuscript.

Appendix 2: Invasion probability of a simple spore killer

Purpose

In this appendix, we give the details for the model presented in Box 2. The calculations are adapted from Desai and Fisher (2007), and give an approximation for the invasion probability of a spore killer with 100% killing efficiency but no killing advantage in a randomly-mating population (i.e., no selfing), starting from a single copy. The spore killer is said to have 'invaded' when it has reached a sufficient copy number so that its dynamics is determined predominantly by the deterministic selective advantage it obtains from killing, rather than by random drift.

Heuristic calculation

As before, let p_D denote the frequency of the spore killer, which we assume to be small ($p_D \approx 0$). Setting $c = 0$ and $e = 1$ in Eq. (A3), we find that the selective advantage of the spore killer is

$$s = \frac{p_D(1-p_D)}{1-p_D(1-p_D)} \approx p_D. \tag{A4}$$

Let N denote the total population size and n the absolute number of copies of the spore killer so that $p_D = n/N$. We now consider a typical change in the allele's copy number due to drift over the succeeding n generations, and compare it to the expected change in copy number due to positive selection on the allele. The reason we consider n generations is that, starting from n copies of the allele, the standard deviation of the fluctuation in allele copy number across n generations that is due to random drift is $\sim n$ (Desai and Fisher, 2007). Therefore, n generations is the timescale for possible extinction of the allele due to random drift. Counteracting this possibility of random loss of the spore killer allele is deterministic selection in favor of it. Across the same n generations, the spore killer has an expected increase in copy number due to positive selection of approximately $ns = np_D = n^2/N$ copies (indeed, slightly more because the selective advantage comes to exceed $s = p_D$ as the spore killer increases in copy number), for a total expected gain of n^3/N copies. Therefore, the deterministic force pushing the spore killer up in copy number dominates the random force that could push it down in copy number when $n^3/N > n$, i.e., when $n > \sqrt{N}$. Thus, the spore killer can be said to have invaded when it has attained $\sqrt{N}$ copies. Because its dynamics before this point is dominated by drift, the probability that it attains $\sqrt{N}$ copies having started as a single copy is approximately $\sqrt{N}/N = 1/\sqrt{N}$. As shown in Box 2 (figure panel a), this approximation accords well with estimates obtained from simulations of the model.

Comparison with a recessive beneficial allele

Consider a recessive beneficial allele D with selection coefficient 1 (i.e., the relative fitnesses of the dd, Dd, and DD genotypes are 1, 1, and 2, respectively; the relevant comparison is to the case of a spore killer with killing efficiency $e = 1$, as considered in the subsection above). From an initial frequency of p_D, the change in frequency of the recessive beneficial mutation across one generation is

$$p'_D = \frac{p_D^2 \times 2 + 2p_D(1-p_D) \times 1 \times \frac{1}{2}}{1+p_D^2} = \frac{p_D(1+p_D)}{1+p_D^2}, \tag{A5}$$

so that the allele's selective advantage

$$s = \frac{p'_D}{p_D} - 1 = \frac{p_D(1-p_D)}{1+p_D^2}. \tag{A6}$$

When $p_D \ll 1$ (the relevant case for invasion), then

$$s \approx p_D, \tag{A7}$$

as for the spore killer considered above Eq. (A4). Thus, although they are not identical, the selective advantages of the spore killer and the recessive beneficial allele with selection coefficient 1 are similar when the two alleles are rare. This explains why the approximate invasion probability derived above for the spore killer resembles the fixation probability for a recessive beneficial mutation with selection coefficient 1 (Kimura, 1962, Eq. 15). It also explains why our result concerning the invasion rate of spore killers in a subdivided population, derived in Box 2, matches the analogous result for recessive beneficial mutations (Gale, 1990, p. 180-181).